Dissertations
Department of Chemistry
University of Eastern Finland

No. 132 (2015)

Janne Salstela

Influence of surface structuring on physical and mechanical properties of polymer-cellulose fiber composites and metal-polymer composite joints

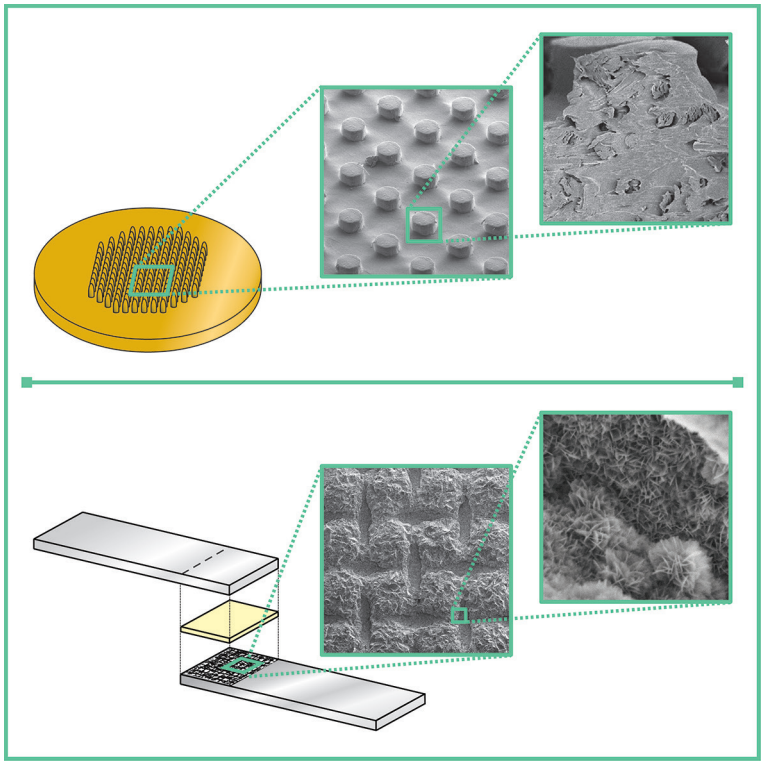

Influence of surface structuring on physical and mechanical properties of polymer-cellulose fiber composites and metal-polymer composite joints

Janne Salstela

Department of Chemistry
University of Eastern Finland
Finland

Joensuu 2015

Janne Salstela
Department of Chemistry, University of Eastern Finland

Supervisors
Prof. Mika Suvanto, University of Eastern Finland
Prof. Tuula Pakkanen, University of Eastern Finland

Referees
Prof. Mikael Skrifvars, University of Borås
Assoc. Prof. Minnamari Vippola, Tampere University of Technology

Opponent
Prof. Jyrki Vuorinen, Tampere University of Technology

To be presented with the permission of the Faculty of Science and Forestry of the University of Eastern Finland for public criticism in Auditorium F100, Yliopistokatu 7, Joensuu, on December 4th, 2015 at 12 o' clock noon.

ISBN: 978-952-61-1968-7 (nid), 978-952-61-1631-0 (PDF)
ISSN: 2242-1033

Grano Oy Joensuu
Joensuu 2015

Abstract

Composites are commonly used materials in applications where the combination of light weight and high robustness is required. Surface structuring is known to have a great influence on the surface functions of the materials. With a proper structure, surface properties such as the wettability, anti-reflectivity and adhesion properties of the materials can be significantly modified. In this study, the frictional properties of the thermoplastic polypropylene/viscose fiber (PP/VF) composites and adhesion in metal-polymer resin composite joints were modified by means of surface structuring.

The main target of the PP/VF-composite research was to study how friction and wear of polypropylene could be affected by addition of viscose fiber as a filler and by microscale surface patterning. The studied polypropylene/viscose fiber-composites were prepared with melt mixing. High adhesion between fibers and PP was ensured by using maleic anhydride grafted polypropylene (MAPP) as a coupling agent. The friction and wear behavior of the micropatterned PP/VF-composites were evaluated under different dry sliding conditions. The high fiber content in the PP/VF-composites was found to enhance considerably the mechanical properties and to lower friction and wear of the specimens in dry sliding. Microstructuring of the PP/VF-composites improved notably the stability of sliding friction and wear properties of the specimens. The cavities between the micro-pillars were observed to behave as “trash cans” where wear debris could accumulate thus stabilizing the sliding system.

The main objective of the aluminum-thermosetting resin studies was to improve adhesion and hence the mechanical strength of the aluminum-polymer resin joints by fabricating micro- and nanoscale surface structures on the aluminum substrate. The surface structures increase the area of adhesion interface and hence promote mechanical interlocking. The surface structures of the aluminum adherends were fabricated with sandblasting, micro-mesh printing and hydration. Two different thermosets (epoxy and unsaturated polyester, UP) were used as adhesives. The chemical interaction between aluminum and adhesives was also enhanced by altering the surface chemistry of aluminum adherends via silanization and plasma treatment. Effects of the surface structures and chemical coupling on adhesion between aluminum and thermosetting resins were evaluated by means of shear strength measurements. Surface patterns in the studied aluminum-epoxy and aluminum-UP joints enhanced the shear properties of the systems significantly. Hierarchy of the surface patterns was found to have a high influence on adhesion. The size of surface patterns has to be optimal for adhesive to penetrate into the formed cavities of the adherend and to form a sufficient adhesion interface with aluminum. Chemical and energetic modifications can improve the wetting properties of hierarchically structured aluminum adherends and hence enhance the shear properties even further.

List of original publications

This dissertation is a summary of joint research publication I and original publications II-III.

I Tarmo Korpela, Janne Salstela, Mika Suvanto and Tuula T. Pakkanen, Periodically micro-patterned viscose fiber-reinforced polypropylene composites with low surface friction, *WEAR* 310 (2014), 20

II Janne Salstela, Mika Suvanto and Tuula. T. Pakkanen, Influence of hierarchical micro-micro patterning and chemical modifications on adhesion between aluminum and epoxy, International Journal of Adhesion & Adhesives, *Accepted for publication 2015*

III Janne Salstela, Jani Tuovinen, Md. Rezaul Karim, Mika Suvanto and Tuula. T. Pakkanen, Influence of multilevel surface structuring and functionalization on adhesion between aluminum and unsaturated polyester, *submitted for publication*

The author's contribution to aforementioned publications:

The key ideas for the topics in **Publications I-III** are based on conversations between supervisors and the author. In **Publication I,** the author manufactured all the measured specimen, performed all the tensile tests and part of the friction/wear tests. The author designed all the surface structuring methods and performed all the experimental work and result analysis in **Publication II.** In **Publication III,** the author played a central role in design of the surface structures, supervising the experimental work and performing the analysis of the results.

Contents

Abbreviations

General:

COF	Coefficient of friction
NFC	Natural fiber composite
RIE	Reactive ion etching
SC	Surface coverage
SEM	Scanning electron microscopy/microscope
TGA	Thermogravimetric analysis
UV	Ultraviolet

Materials:

GPTM	3-Glycidoxypropyltrimethoxysilane
IPDA	Isophorondiamine
MAPP	Maleic anhydride grafted polypropylene
MPS	3-Methacryloxypropyltrimethoxysilane
PP	Polypropylene homopolymer
UP	Unsaturated Polyester
VF	Viscose fiber

1. Introduction

The growing need to make everything faster, stronger or more efficient has driven scientists to develop high performing materials such as polymers and composites. Polymers are typically used in applications where properties such as lightness, flexibility of design, good resistance to chemicals and low costs are needed.[1-3] Composite materials, which are a combination of two or more immiscible materials, have the best characteristics of each of its components and the sum of characteristics that none of the individual components possess.[4,5] Composite materials are widely used in sports equipment, aircrafts, high performance cars and in all other applications where low weight and high robustness are desired.

Surface structure is known to have a great impact on the properties of materials. With a proper surface structure the material can have features that it does not possess on its own. The water repellent and self-cleaning surface of lotus leaf is probably the most referred to in discussions of functional hierarchical surface structures[6-8] (Fig. 1. A). In nature plants, animals and insects are known to have many superior surface properties such as hydrophobicity[8-10], anti-reflectance[11] and high, but yet reversible, adhesion[12-14]. These properties scientists have tried to replicate to man-made materials. Surface structuring is known to affect greatly also on the material properties such as friction and wear[15,16] and shear strength.[17] Tread patterning of vehicle tires is a good example of modifying the surface of a man-made material in order to achieve better surface properties such as enhanced friction (Fig. 1. B).[18] In the forthcoming chapters, the following topics including polymers, surface structuring, composite systems, tribological and mechanical testing methods are introduced.

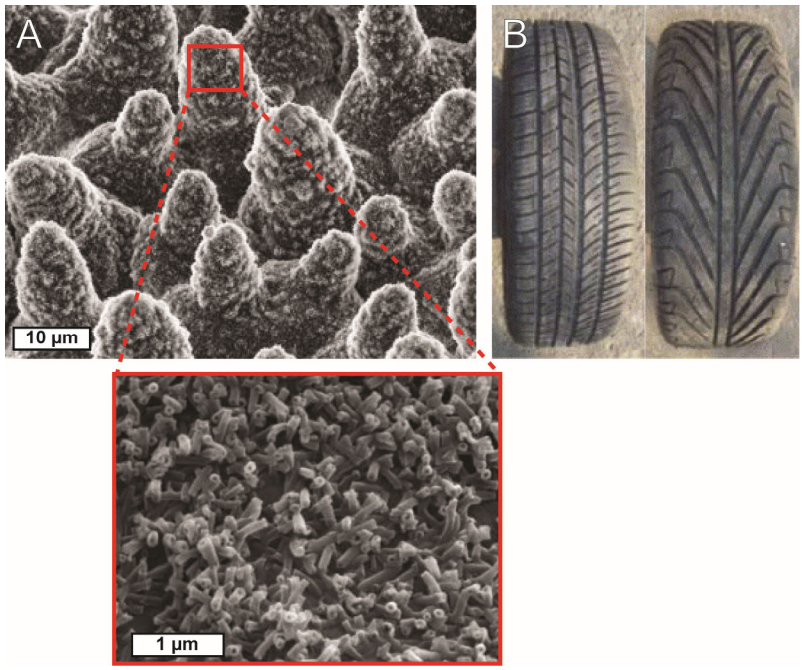

Figure 1. A) Hierarchical surface structure of lotus leaf [19] (modified) and B) tread patterning of vehicle tire[18] (modified).

1.1. Polymers

Polymers are typically organic compounds based on carbon, hydrogen, oxygen, nitrogen, silicon, and other nonmetallic elements. Commonly they have a backbone of carbon atoms in a form of long chainlike structure. Polymers are formed through polymerization where the starting materials, monomer molecules, take place in chemical reaction resulting in polymer chains or three-dimensional network. Familiar examples are polypropylene, polyethylene, nylon, poly(vinyl chloride), silicone rubber and resins such as epoxies and urethane foams. Polymers have typically low densities, low electrical conductivities and low stiffness and strength when compared to more traditional materials such as metals and ceramics.

1.1.1. Thermoplastics

Thermoplastics are high molar mass polymers having linear or branched structures.[20,21] They are flexible and have an ability to soften and to harden reversibly by changing the temperature. This enables an easy molding procedure and reusability.[1,21] Thermoplastics are widely used in children's toys, optical applications (lenses, cds, dvds etc.), containers, kitchenware, pipes and in many other everyday applications.

1.1.2. Thermosets

Thermosets are a group of prepolymers or resins which transform into a cross-linked product when they are mixed with a suitable curing agent or initiator and are then typically cured by applying elevated temperature or ultraviolet light.[1,21] Because of their network structure, thermosets have a very high tolerance to chemicals and they cannot be softened by heat. With excess heating, the cured thermosets start to decompose.[21] Thermosets are generally used as adhesives, coatings and matrix materials in fiber reinforced composites.

1.2. Surface structuring

With surface structuring, materials can have surface properties that would not otherwise be present. Several studies have been made, where hierarchical surface structures causing self-cleaning and superhydrophobic properties have been manufactured to polymer materials.[22-25] In adhesion studies, the high dry adhesion properties of gecko and insect feet[12-14,26] have inspired scientists to reproduce their surface structures in order to achieve these properties in artificial materials (Fig. 2).[27-29]

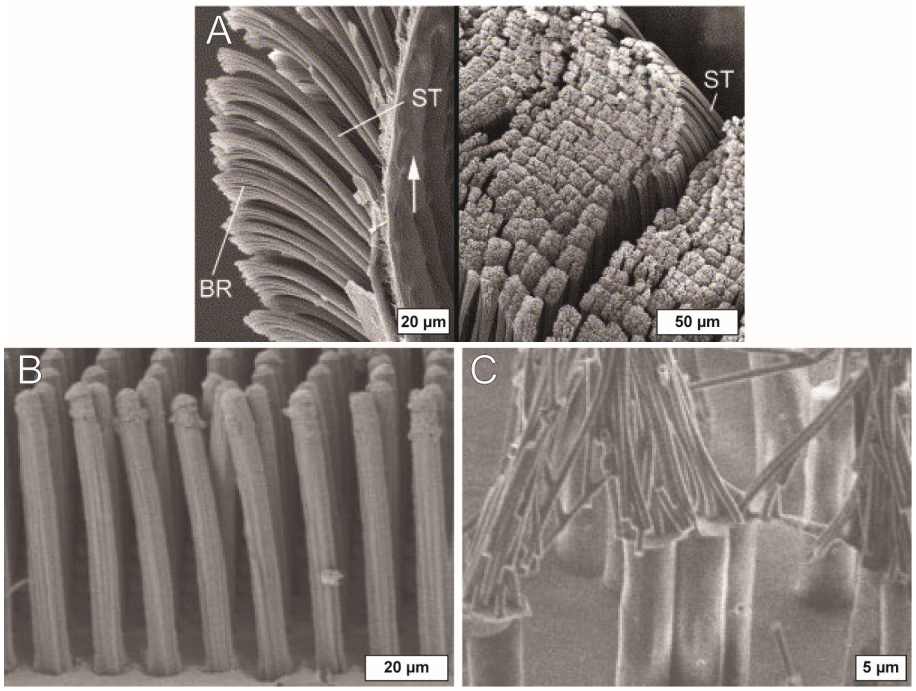

Figure 2. SEM images of A) surface structure of gecko feet[12] and gecko-inspired B) polyurethane microarray[27] and C) hierarchical polyethylene nanofiber structures[28].

In order to achieve functional surface structures, a vast variety of different methods have been proposed[10,24,25,30-35]. Because of the complexity of multilevel hierarchical surface structures, fabrication requires typically a multistep process. With polymers, the structures can be fabricated for instance via direct replication of plant leaves and insect wings, but typically they are fabricated with thermal imprinting and mold casting. A mold having a negative functional surface structure is first fabricated, followed by mold casting where the positive surface structure is produced to a polymer surface. Surface structures can be achieved e.g. by duplicating the textures from nature's organisms[10,34,35] or by combining different micro- and nanostructuring methods[24,25,33]. When a functional surface structure is desired on a metal surface, direct modification methods are typically used. Direct methods consists of e.g. plasma, etching, hydration and mechanical roughening methods[36-40]. Compared to the replication methods, the direct methods are usually difficult to apply in mass-production.

1.3. Cellulose fiber composites

In order to reduce raw material costs and increase the mechanical properties of polymers (phenol- or melamine-formaldehyde resins), the industry have been applying the cellulose fibers as an inexpensive filler material since early 1900s.[41] Cellulose fibers can be used in their natural form (cotton, jute, sisal)[42-48], but also modified cellulose fibers have been used if improved physical properties or good processability are required.[49,50] The chemical structure of cellulose is presented in Fig. 3A.

Cellulose fiber composites consist of a polymer matrix and cellulose fibers as a reinforcing filler.[51,52,53] Cellulose fiber composites are a subclass of natural fiber composites (NFC). Because of the environmental and economic benefits of NFCs, they are replacing in increasing volume the conventional composite materials (glass/carbon polymer composites) in various applications including packaging, furniture, automotive industries, building, and insulation materials.[54-57] The use of NFCs has many benefits, such as a decrease in the raw material cost, enhanced physical properties, a low density, and environmental friendliness.[54,58]

When the cellulose fibers are compounded with polyolefins such as polyethylene or polypropylene, a suitable coupling agent is typically needed.[59-62] The hydrophobic nature of polyolefins results in poor connection to the hydroxyl groups of the cellulose chains. To achieve higher adhesion between polymer and cellulose fiber, coupling agents are added as the third component in the composite. The coupling agents must have chemical groups that can chemically bind to the alcohol groups of cellulose chain and a backbone that is compatible with the matrix polymer used. Most common coupling agent in cellulose fiber composites are polymers containing maleic anhydride groups (Fig. 3B)[59,61,63]. Other typical coupling agents are e.g. organosilanes[62,64] and acetic anhydride[65] that are used to modify the cellulose chains.

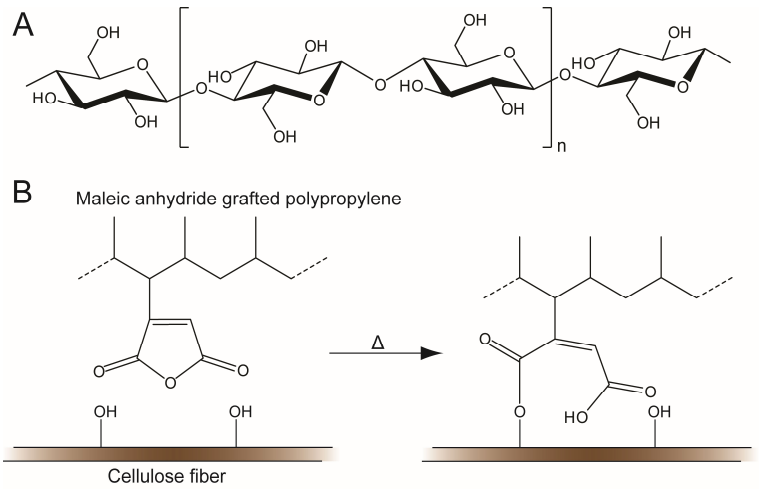

Figure 3. A) Chemical structure of cellulose chain and B) the esterification reaction of its hydroxyl groups with maleated polypropylene.[60]

1.4. Metal-polymer resin composite joints

In metal-polymer resin composite joints, or shortly **adhesive joints**, polymer resin (adhesive) is joining two metal substrates (adherends). In the automotive and the aerospace industries, adhesive joints are widely replacing the conventional welding and mechanical (bolt-nut, rivet) joints.[66-68] Adhesive joints have many advantages such as fast and easy manufacturing process, lightness, flexibility of design, capability to join dissimilar materials and uniform load distribution over the whole bonded area.[68-70] As any other joining method, adhesive joining methods have some disadvantages such as required thermal curing, environmental stress caused by the use of chemicals, and the limited shelf life of adhesives.[71]

1.4.1. Adhesion mechanisms

Adhesive joints fail typically from the interface of the adhesive and substrate (adhesive failure). The failure can also be cohesive where either the adhesive or substrate fails. In order to fully understand why the adhesive joints fail, it is essential to know the phenomena behind adhesion. Adhesion can simply be described as a sum of forces keeping two surfaces together. Adhesion phenomenon is a complex combination of physical and chemical interactions. Several mechanisms for adhesion have been proposed.[66,72,73]

One of the oldest adhesion mechanism theories is **mechanical interlocking**. According to the theory, adhesion is caused by the fusion of adhesive and substrate. Adhesive penetrates into the dents, holes and cavities of the substrate, causing so called interlocking points. Mechanical interlocking is an important phenomenon when rough materials such as wood and textiles are bonded adhesively. However, it does not explain why smooth materials (glass, metals, polymers, and ceramics) can have strong adhesion to adhesives. Chemical bonding or **chemisorption** is a generally accepted theory explaining this behavior. In the theory, adhesive and substrate are close enough to form chemical bonds (covalent, ionic and metal-metal bonds) between the two interfaces. Mechanical interlocking and chemical bonding are illustrated in Figure 4.

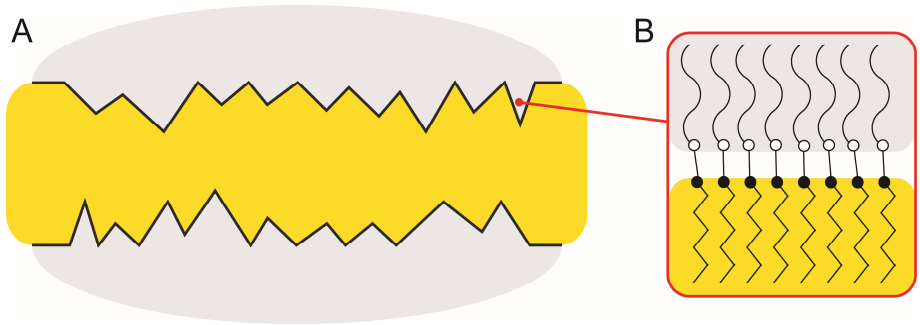

Figure 4. A schematic illustration of A) mechanical interlocking and B) chemical bonding.[66] Yellow color represents adhesive and light gray the substrate.

Other proposed adhesion mechanism theories are **physisorption**, **diffusion** and **electrostatic theories**. In physisorption theory, the adhesion is caused by the secondary bonds (van der Waals interactions, hydrogen bonds and acid-base interactions). Diffusion theory can explain adhesion systems where both components are polymers that are mobile and miscible. Polymer chains of the components get entangled and a mixture of the two polymers is formed on the interface. Electrostatic theory is one of the newest theories of adhesion and is based on the formation of electrostatic charges of opposite signs that attract each other.

1.4.2. Epoxy adhesives

Epoxy resins are thermosetting polymers that are widely used as coatings, matrix materials in composites, and as adhesives.[74] Typically epoxy resins are synthetized in step-growth polymerization from epichlorohydrin and phenols. The resulting resins are structurally ethers and have epoxy groups in the end of polymer backbone (Fig. 5.) The epoxy resin is most commonly cured in a reaction using acid anhydrides or diamines as curing agents at elevated temperatures.[74-77]

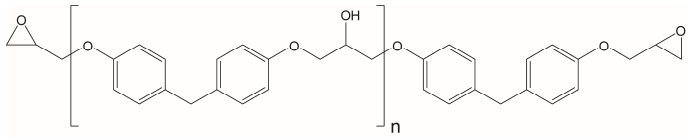

Figure 5. Chemical structure of bisphenol F and epichlorohydrin based epoxy resin.

Because of their chemical structure containing different functional groups, epoxies have high adhesion properties to a wide variety of materials such as metals, wood, polymers and ceramic materials and therefore it can be used to join different material pairs.[68,76] Epoxies have good characteristics such as excellent resistance to chemicals and elevated temperatures, and great toughness.[68,75-77]

1.4.3. Unsaturated polyester (UP) adhesives

Due to inexpensiveness, easy handling, good chemical and mechanical properties, unsaturated polyester (UP) resins are widely used as coatings and as the polymer matrix in composites.[78-82] Like epoxies, UP resins are thermosetting polymers. Unsaturated polyester resins are generally prepared in condensation reaction of saturated and unsaturated dicarboxylic acids with glycols.[75] In general, UP resin (Fig. 6.) is cured in free radical addition copolymerization in the presence of vinylic comonomer such as styrene.[83,84]

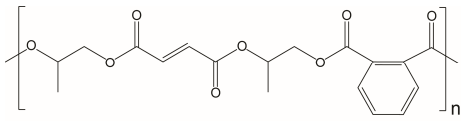

Figure 6. Chemical structure of UP resin based on maleic anhydride, phthalic anhydride and 1,2-propanediol.

1.4.4. Enhancement of adhesion in metal-thermosetting resin composite joints

Because of adhesion weakening interfaces (air pores, grease and other contaminants)[72], metal adherend surfaces have to be finished in a way that proper adhesion can be achieved.[71,85,86] The adhesion promoting surface treatment methods can be roughly categorized into **mechanical**, **chemical**, and **energetic** surface treatment methods.[86]

Mechanical surface treatment methods are used to increase the contact area of metal surface, to achieve more locking points on macro- and microscale via roughening the surface, and in the case of aluminum, to remove the oxide layer.[67,87,88] Typical mechanical surface treatment methods are grit/sand blasting[87,89], mechanical abrasion with sandpaper[86] and groove fabrication[17].

The common chemical surface treatment methods used for metals are acid etchings[67,85,90], anodizing[91,92] and chemical coupling[93-95]. They can produce micro-nanoscale surface roughness and/or functionalize metal adherend surface. Modification of the adherend surface with organosilanes as coupling agents has been proven to be an effective way to increase adhesion in metal-polymer resin systems. Silane has to have suitable functional end groups in its structure in order to act as a chemical bridge between the substrate and adhesive. In silanization, the silane binds to the substrate surface leaving its other reactive end group free for adhesive. The chemical reactions in silanization are illustrated in Figure 7.

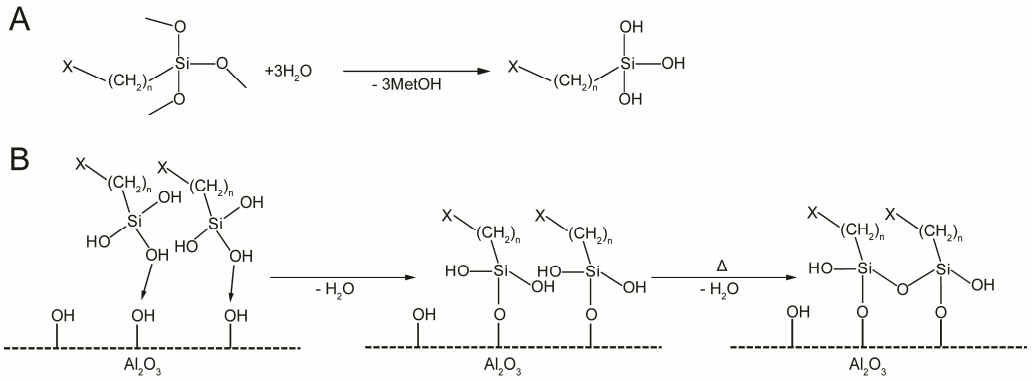

Figure 7. A) Hydrolysis of organosilane and B) the reactions of hydrolyzed organosilane on the aluminum/Al_2O_3 surface.[96-98]

Energetic surface modification methods (laser texturing, flame, plasma)[67,99,-102] have been studied as environmentally friendly alternatives to modify the morphology and chemistry of adherend surfaces and to remove organic impurities. The plasma treatment of metal surface has been presented to be an effective adhesion promoting technique also for metal-polymer resin interfaces.[103-106] In plasma treatment, the substrate is bombarded with plasma gas containing ions, radicals and electrons. The surface chemistry of the substrate can be altered by using different reaction gases. Plasma treatment can also be used for etching the surface of substrate, leading to modified topography of the surface. In the case of aluminum substrate, the oxygen plasma treatment oxidizes aluminum surface leading to better wetting and adhesion properties.[104]

1.5. Tribological studies

Tribometers are devices that are used to measure friction and wear under controlled conditions. The set-up is selected to match the frictional environment of the application system as closely as possible.[107-109] A poorly chosen tribometer system can provide misleading results. On laboratory scale, the three mostly used types of tribometers are **pin-on-disk**, **pin-on-flat**, and **block-on-ring** (Fig. 8). The friction force F_T in these tribometers is typically measured with sensitive force sensors. Either the force needed to maintain the sliding at constant speed or the extent of deceleration of the test system by the contact can be measured. The applied normal load F_N is typically determined with load cells or by applying a known load to the friction system. The friction coefficient μ is obtained by dividing the counteracting friction force F_T with the applied normal load F_N:

$$\mu = F_T / F_N \qquad (1)$$

Wear of the sample can be measured in several ways. The extent of wear can be expressed as **lost mass** or **lost volume**. The lost mass is measured by simply weighing the sample before and after the tribological measurement. Usually, lost volume is expressed as the *specific wear rate* W_S:

$$W_S = \textit{Lost volume} / (\textit{Load} * \textit{Distance}) \qquad (2)$$

The stable friction coefficient and the specific wear rate values achieved from the tribological studies tell very little of the actual system because the operating environment affects greatly the system. Therefore it is essential to report all the variables (humidity, temperature, atmosphere) having influence on the sliding process.[107,110,111]

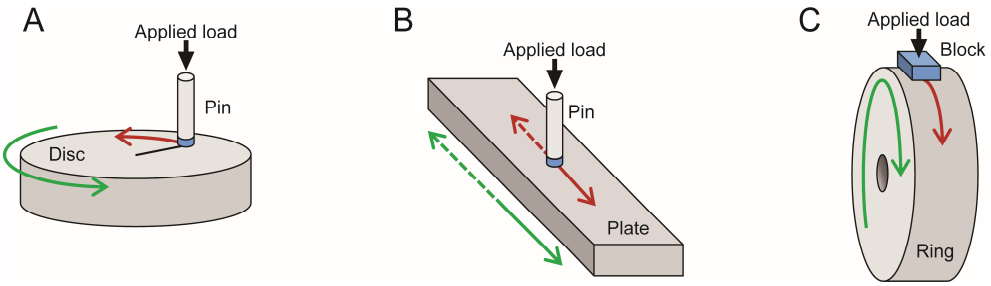

Figure 8. Schematic images of a A) rotating pin-on-disk, B) reciprocating pin-on-flat, and C) rotating block-on-ring tribometer geometries. The green arrow indicates the movement of the counter surface and the red arrow indicates the friction force.[112-114]

1.6. Shear and tensile strength studies

1.6.1. Shear testing

When the strength and durability of metal-polymer resin composite joints is of interest, these properties are typically tested with shear strength studies. The geometry of the shear strength measurement has to be selected in a way that it represents the practical application of interest. Destructing forces in the tests should represent those that are present in the application during its life cycle. Typical laboratory scale shear strength tests for adhesive joints are **lap-shear** and **wedge-crack** tests.[115-118] The simplified schematic illustrations of these systems are presented in Figure 9.

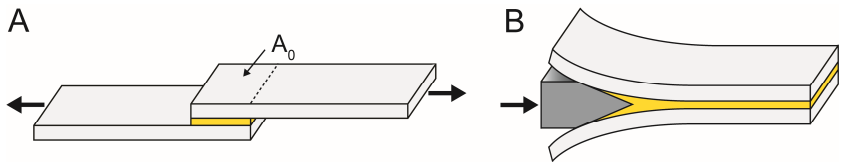

Figure 9. Schematic illustrations of A) a single-lap-shear and B) a wedge-crack test configuration. Adherend surfaces are indicated with light gray and adhesive with yellow color. Black arrows indicate the directions of the applied stress.

Single-lap-joint shear strength tests are typically carried out as short-term dynamic tests where the loading force is increasing constantly. In dynamic lap-shear tests, the shear strength τ is obtained by dividing the maximum applied stress F_{max} with the surface area of the joint A_0: [119]

$$\tau = F_{max} / A_0 \qquad (3)$$

Wedge tests, instead, are typically long-term static force tests, where the wedge is driven into the bond line of a flat-bonded specimen with a constant force and the specimen is exposed to humid/hot-wet atmosphere.[117,118] There are also variants of the lap-shear and wedge-crack techniques, where for instance the applied stress (periodical loading/unloading, constant force, constantly increasing force) or the test geometry (double-lap-joint shear test, tapered double cantilever test, peel test, pull-out test) are different from those mentioned above.

1.6.2. Tensile testing

The mechanical properties of polymers and their composites are typically obtained via tensile testing where a dynamic load is applied on a tensile specimen. The typical geometries of the tensile specimens are circular or rectangle rods.[120] A schematic illustration of a typical tensile specimen used for polymer materials is presented in Figure 10.

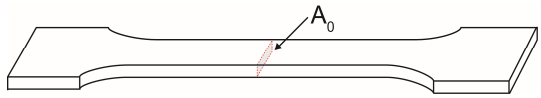

Figure 10. Schematic illustration of tensile test specimen.

From tensile tests, properties such as Young's modulus E, maximum tensile strength R_m and elongation at break can be deduced. The tensile strength R_m is obtained by dividing the maximum applied stress F_{max} with the original cross-sectional area A_0, similarly as in equation (3).

For materials whose elastic portion of stress-strain curve is not linear (e.g. many polymers, gray cast iron, concrete), the Young's modulus (elastic modulus) E is determined either as *tangent* or *secant modulus*. The *tangent modulus* is taken as the slope of stress-strain curve at some specific level of stress (typical strain value 0.02-0.1%). The *secant modulus* is obtained from the slope of a secant drawn from the origin to some given point of the stress-strain curve.

1.7. Aims of the study

Polymer composites and composite joints are nowadays used widely in automotive or aerospace industries. Physical and mechanical properties of the composites and composite joints play an important role since wear and/or fractures can cause a catastrophic failure, therefore the need for high performance materials is growing. This research focuses on improving the mechanical and physical properties of composites by altering their surface structures with methods that can be easily scaled to industrial scale. The use of chemical surface modifications for enhancement of adhesion in composite joints is also investigated. The specific objectives of this study are as follows:

1. To find out how the micro-pillar surface structures affect the friction and wear behavior of cellulose fiber-reinforced polypropylene composites.

2. To study how the microscale mesh structuring and hierarchical micro-micro surface structuring of aluminum adherend influence adhesion in aluminum-epoxy composite joints. Influence of silanization and plasma treatment on adhesion will also be examined. Moreover, the effects of various combinations of the modifications will be studied.

3. To examine the effect of the superimposed micro-nano surface structures on adhesion in aluminum-unsaturated polyester resin composite joints. Enhancement of adhesion between nanostructure and unsaturated polyester resin by silanization will also be searched.

2. Experimental

The materials, micro- and nanostructure fabrication, and characterization methods used in this research are described on a general level for all studied systems. Experimental parameters such as the microstructuring parameters, the shape of patterned areas, injection molding parameters, curing conditions of the resins, and plasma treatment parameters are described in detail in publications I-III.

2.1. Materials

Studies on friction and wear behavior of cellulose fiber composites were carried out with a mixture of isotactic polypropylene (PP, HD 120 MO) and viscose fiber (VF, Danufil® KS, 10-20 μm in diameter). The PP was acting as the matrix material and VF as the reinforcing filler material. Maleic anhydride grafted polypropylene (MAPP, Polybond 3200) was used as a coupling agent. The amount of added viscose fiber ranged from 10 w-% to 40 w-%.

The shear stress studies of the aluminum-polymer resin composite joints were performed with commercial EN AW-5754-aluminum acting as the adherend material. Araldite GY 285 bisphenol F epoxy resin (Huntsman) and Synolite 8388-P-1 unsaturated polyester resin (UP, blended with styrene, DSM composite resins) were selected as adhesives. Epoxy resin was cured with isophorondiamine (IPDA, ≥ 99 %, Sigma Aldrich) and UP resin with methyl ethyl ketone peroxide as a curing agent (Butanox M50, S.A. AkzoNobel Chemicals N.V.). The relative amounts of the curing agents to the resins were 24.8 w-% and 2 w-%, respectively.

The chemical coupling of the aluminum adherend and adhesives was performed with 3-glycidoxypropyltrimethoxysilane (GPTMS, ≥ 98 %, Sigma Aldrich) and 3-methacryloxypropyl-trimethoxysilane (MPS, 98 %, Sigma Aldrich). The former was used with epoxy adhesive and the latter with UP adhesive. The chemical structures of the silanes are presented in Figure 11.

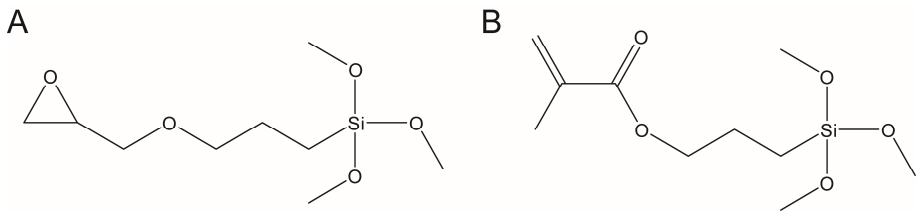

Figure 11. Chemical structures of A) 3-glycidoxypropyltrimethoxysilane (GPTMS) and B) 3-methacryloxypropyl-trimethoxysilane (MPS).

2.2. Fabrication of the surface structures

The specimens of PP/VF-composites possessing micro-pillar surface structures were manufactured with injection molding using microstructured mold inserts. The mold inserts were generated from aluminum foils by using a micro-working robot (Fig. 12A) followed by fixing the aluminum foil onto a steel support with super glue (Fig. 12B). The micropatterned PP/VF-composite specimens were manufactured via melt mixing and injection molding by using the fabricated insert molds and a laboratory scale injection-molding machine having a separate twin-screw melt compounder (Figs. 12C and 12D).

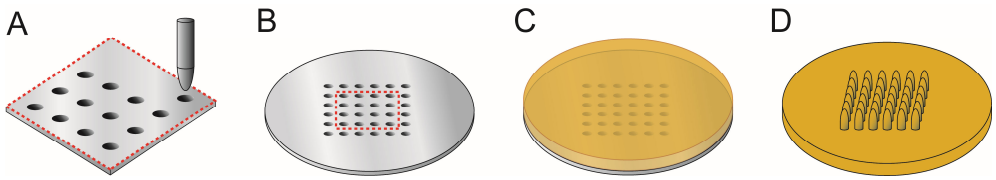

Figure 12. Sequential illustration of fabrication of microstructured PP/VF specimens: A) fabrication of mold with a micro-working robot, B) the micropatterned aluminum mold, C) the injection molding sequence and D) the final injection molded PP/VF-specimen.

In aluminum/polymer resin composite joints, the microscale surface structures were manufactured directly onto aluminum adherends with a micro-mesh printing technique (Fig. 13) and/or sandblasting. Micro-mesh structures were obtained with stainless steel microscale meshes (mesh sizes of 100µm, 200 µm and 400 µm) by using a hydraulic press. Sandblasting was performed by using a sandblasting equipment with quartz sand (grain size > 1mm). The nanoscale surface structure of aluminum adherends was obtained via hydration under boiling deionized water.

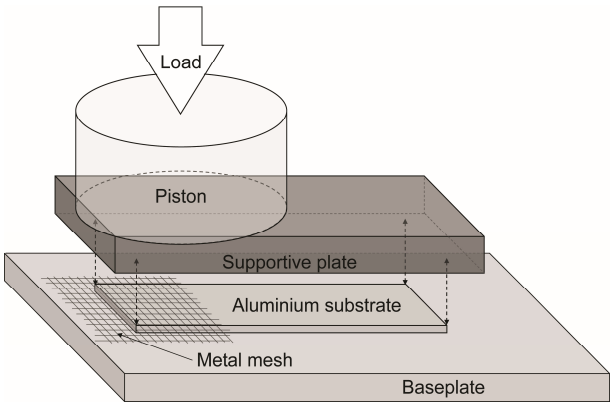

Figure 13. An illustration of micro-mesh printing technique.

2.3. Tribological measurements

The friction and wear measurements of PP/VF-composite specimens were executed with a pin-on-disk tribometer by using two different linearly ground stainless steel discs as counter surfaces. In the pin-on-disk measurements, the samples were fixed on the pin so that the patterned side of the samples faced the counter surface with a constant load of 2 N. One of the counter surfaces had low and the other high arithmetic roughness values (R_a 0.1 and R_a 1.5) in order to promote adhesive and abrasive wear of the PP/VF-specimens. The pin-on-disk method was selected because it allows measuring friction and wear properties in continuous, uninterrupted sliding.

Wear and friction of the PP/VF-composite specimens were measured and analyzed after the stable sliding conditions were achieved. Wear of the samples were measured by monitoring changes in the vertical position of the sample holder pin. During the measurements, wear of steel counter surfaces was considered to be negligible. Therefore the vertical deviation of the sample pin was considered to give wear of the composite samples in one dimension which was then used to calculate the specific wear rate W_s [mm^3/Nm]:

$$W_s = h * A_p * Load^{-1} = h * SC * A * Load^{-1} \quad (4)$$

where h is the slope of the height loss curve in the analyzed distance [10^{-3} mm/m], A_p is the true contact area of specimen [mm^2] and *Load* is the applied normal load during the measurement [N].

The true contact area A_p is obtained from the structured surface area of the sample pin A and the surface coverage SC. The surface coverage SC [%] of the samples having micro-pillars arranged in a square lattice form is calculated on the basis of the separation of micro-pillar centers W and diameter of the micro-pillar tops T (Figure 14):

$$SC = (\pi/4) * ((T / W)^2) \quad (5)$$

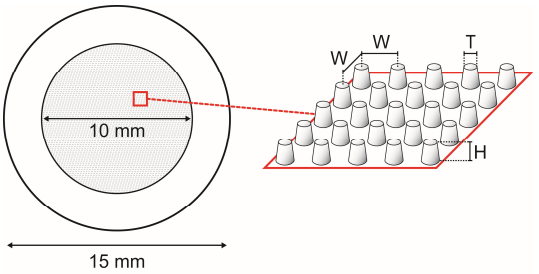

Figure 14. Scheme of a PP/VF-composite sample pin. Light gray color indicates the patterned area A and white color the unpatterned area. W = distance between two micro-pillars in the grid, T = top diameter of the micro-pillars and H = height of the micro-pillars.

2.4. Tensile and shear strength measurements

The mechanical properties of the PP/VF-composites and aluminum-polymer resin composite joints were determined by using material testing machine with 1 kN and 10 kN load cells, respectively. The mechanical testing was performed with a tensile test for PP/VF-composites and with a lap shear test for the aluminum-polymer resin composite joints. The geometries of the mechanical testing specimens are shown in Figure 15.

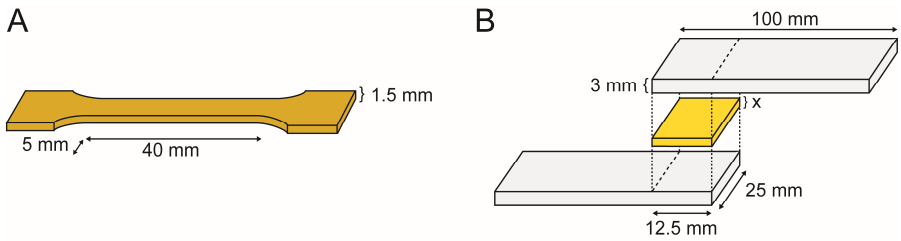

Figure 15. Schematic image of A) tensile test and B) single lap shear test specimens. Thickness of the adhesive layer (x) is 0.2 mm with epoxy and 0.1 mm with UP.

The tensile test specimens, made via injection molding, were fastened to the material testing device by using symmetric grips. Fastening of the single lap shear test specimens was done with asymmetric grips for a proper alignment of the specimens.

2.5. Other characterization methods

The compositions of the PP/VF-composite samples were studied with thermogravimetric analysis (TGA). The TG analysis was possible because viscose fibers and PP-matrix are decomposing in different temperature ranges. Scanning electron microscopy (SEM) was used to monitor the quality of manufactured surface structures on the PP/VF-composite specimens and aluminum adherends. A thin layer of gold was sputtered on all of the samples to prevent charging during the SEM imaging.

Cross-sections of the patterned PP/VF-composite samples were imaged with SEM to study the orientation and distribution of viscose fibers in the micro-pillars and in the bulk. The worn PP/VF-composite samples were analyzed also with optical microscopy, which enabled more detailed imaging of the viscose fibers compared to SEM.

To gain micro- or nanolevel fracture information, the fractured surfaces of the aluminum-polymer resin composite joints were examined with SEM. The visual appearances of the fractured single lap joint specimens were captured with a camera either under normal or ultraviolet (UV) light. Fracture analysis by imaging under UV light was used with the aluminum-UP resin composite joints, because the fluorescence of UP enabled more rigorous observation of the UP residues.

3. Results and discussion

3.1. Influence of microstructuring on friction and wear of viscose fiber/PP composites [I]

The main target of the PP/VF-composite research was to study how friction and wear of polypropylene could be affected by addition of VF as a filler and by microscale surface patterning. The research was based on a previous study[15] where the dry sliding properties of PP were adjusted with micro-pillar structuring. PP micro-pillars were found to wear significantly during the sliding. For the present study, more robust PP/VF-composites were selected as the material. Pure PP was chosen as a reference material to which the PP/VF-composites were compared. Relatively smooth (R_a 0.5) and rough (R_a 1.5) steel discs were chosen as counter surfaces in order to find out the behavior of PP/VF-composites in two different wear environments.

3.1.1. Composition and mechanical properties of the viscose fiber/PP composites

Viscose fiber compositions of the PP/VF-composites were analyzed with thermogravimetric analysis (TGA). According to a previous study[61], the viscose fiber content of a PP/VF sample can be acquired in TGA as a relative weight loss within the decomposition range of viscose fiber (200-400 °C). The weighed PP, VF and MAPP mass fractions and the measured VF contents of the PP/VF-composites are shown in Table 1.

Table 1. Weighed and measured compositions for the PP/VF-composite series.

Series	Matrix composition PP/MAPP [%]*	Weighed VF [%]	Measured VF [%]
PP/VF10	89.4/0.6	10	10.0
PP/VF20	78.8/1.2	20	18.9
PP/VF30	68.2/1.8	30	29.6
PP/VF40	57.6/2.4	40	36.1

* PP and MAPP formed the matrix fraction

In addition to the patterned specimens, tensile test specimen were manufactured for each composite series to determine their mechanical properties via tensile testing. The mechanical testing results of the PP/VF-composites are shown in Table 2.

Table 2. Measured mechanical properties of the studied PP/VF-composite series.

Series	E [GPA]	R_m [MPa]	ε [%]
PP	2.9 ± 0.2	40.7 ± 1.5	45.1 ± 8.3
PP/VF10	3.2 ± 0.5	40.9 ± 1.7	14.6 ± 2.6
PP/VF20	3.2 ± 0.2	47.8 ± 1.2	7.7 ± 0.7
PP/VF30	3.9 ± 0.4	55.5 ± 1.5	6.4 ± 0.4
PP/VF40	4.7 ± 0.5	71.1 ± 3.3	5.7 ± 0.8

E: Young's modulus R_m: Tensile strength ε: Elongation at break

3.1.2. Microstructures

The micropatterns of the PP/VF-composites were fabricated according to the previous study.[15] All micro-pillars were in a square lattice arrangement with surface coverages (SC) ranging from 15 to 45 %. All micropatterns were fabricated with the micro-working robot using a tungsten carbide needle with a tip diameter of around 100 µm. After the injection molding, the dimensions of the microstructures on the specimens were determined with SEM. The dimensions of the microstructures are listed in Table 3.

Table 3. Set and measured micropattern parameters.

	Set parameters		Measured parameters		
Pattern	SC [%] [a]	W [µm] [b]	T [µm] [c]	SC [%]	A_p [mm^2] [d]
SC15	15	229	106 ± 2	16.8 ± 0.5	13.2 ± 0.4
SC25	25	177	104 ± 4	26.9 ± 2.1	21.1 ± 1.6
SC35	35	150	104 ± 4	37.8 ± 2.6	29.7 ± 2.0
SC45	45	132	105 ± 6	49.2 ± 5.3	38.7 ± 4.1

[a] Target SC of the micropatterns.
[b] Distance between two micro-pillars in the grid.
c Top diameter of the micro-pillars.
[d] Contact area of the micropattern; A_p = SC x patterned area of the pin

Target height of the micro-pillars in patterned area of all samples was set to be 50 µm and based on SEM images, the height was estimated to be 49 µm. A schematic presentation of the micropatterned composite specimen is shown in Figure 14 and examples of the fabricated micropatterns are shown in Figure 16.

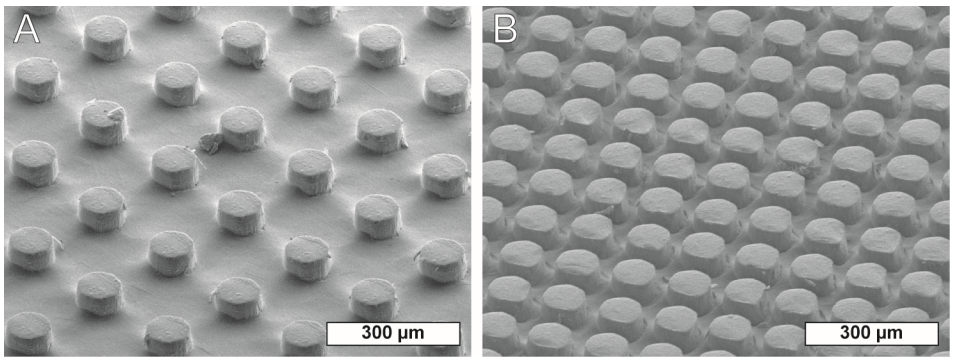

Figure 16. SEM images of A) SC15 and B) SC45 micropatterns on PP surface.

In the following results, SC100 surface refers to an unpatterned surface to which the micropatterned surfaces were compared to.

3.1.3. Friction and wear of microstructured viscose fiber/PP composites

During the friction and wear tests, all of the micropatterned surfaces of PP/VF-composites showed shorter run-in period and much less fluctuation in the sliding friction coefficient when compared to the unpatterned surface (Fig. 17).

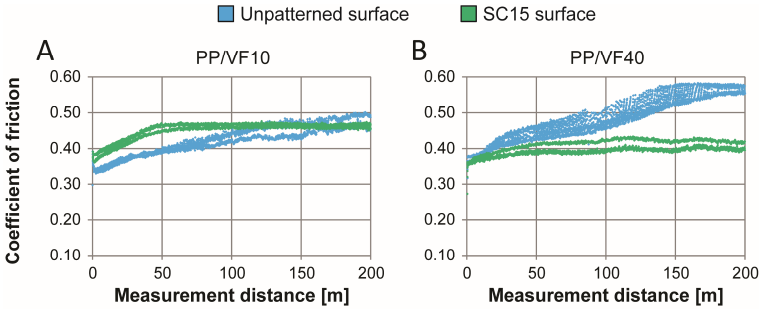

Figure 17. Friction behavior of unpatterned and patterned (SC15) PP/VF10 (A) and PP/VF40 (B) sample surfaces sliding against rough counter surface.

Figure 18 shows how wear debris have piled up into the cavities between the micro-pillars, leaving the tips of the micro-pillars clean during the formation of the transfer layer. On the unpatterned surface the debris stayed between the sliding PP/VF-composite and the counter surface as a transfer layer, causing more unstable friction behavior (Figs. 17 A and B). The ability of SC15 samples to collect the debris was most probably the cause of the friction stabilization. Same kind of effect was also seen in the previous study.[15]

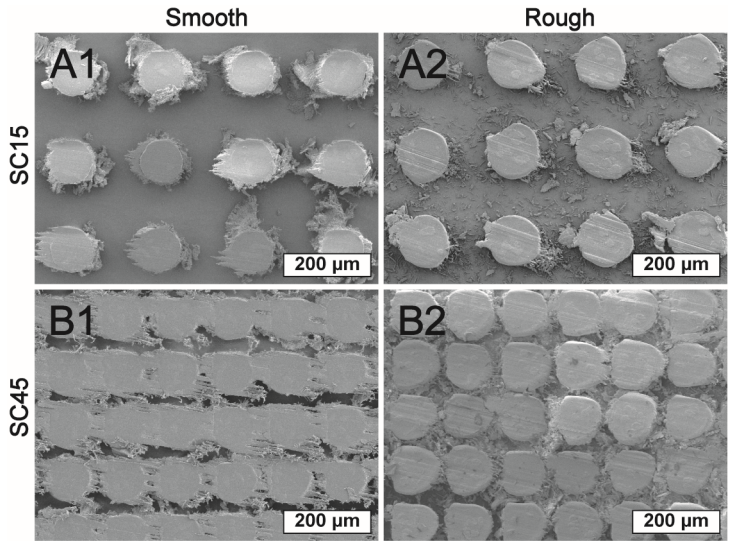

Figure 18. SEM images of worn PP/VF40 samples with the surface coverage of A) SC15 and B) SC45, slid against 1) smooth and 2) rough steel counter surfaces.

It is also noticeable how the smooth counter surface caused creeping or adhesive wear (Figs 18 A1 and B1) whereas the rough counter surface promoted the abrasive wear mechanism with flaking and micro-cutting (Figs 18 A2 and B2).

The measured stable friction coefficient and wear values of PP (reference), PP/VF10 and PP/VF40 series against the smooth and rough steel counter surfaces are shown in Figure 19. The friction and wear rate values of PP/VF20 and PP/VF30 series were between those of PP/VF10 and PP/VF40 and therefore they were excluded from Figure 19 for clarity.

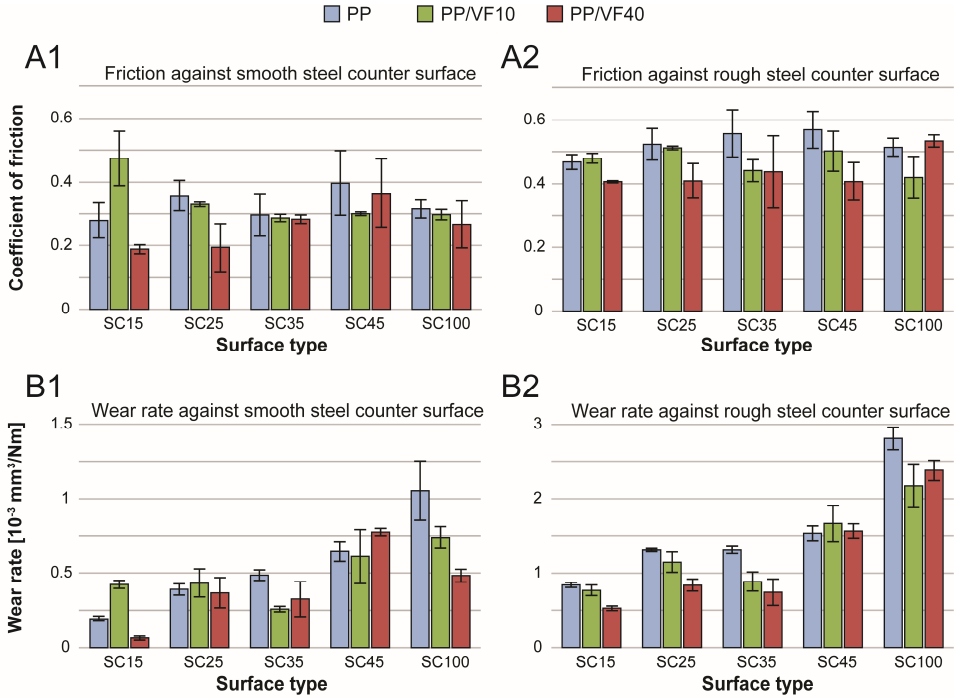

Figure 19. Measured stable A) friction levels and B) wear rates for the PP, PP/VF10 and PP/VF40 specimens against 1) smooth and 2) rough steel counter surfaces.

Overall, the friction levels of the test specimens slid against the smooth counter surface were lower compared to those slid against the rough counter surface (Figs 19 A1 and A2). This was most probably due to the high roughness of the counter surface, which led to an increased mechanical resistance and therefore to higher friction between the specimen and the steel surface. When the micropatterned specimens were slid against rough steel counter surface, the increasing viscose fiber content resulted in lower friction (Fig 19 A2). Most probably, the high viscose fiber content in the micro-pillars and the higher stiffness of the composite material (Table 2) resulted in decreased adhesion between the counter surface and the micro-pillars and hence lower friction.

When slid against the smoother counter surface, the wear rates of the different materials are affected only slightly by the micropatterning (Fig 19 B1). In contrast, when the specimens are slid against the rougher counter surface, more noticeable results can be seen as the decreasing SC value reduces significantly the wear rate compared to unpatterned surfaces (Fig 19 B2). Reduced

wear in the presence of low surface coverages is most likely due to the larger cavities between the micro-pillars. Wear debris can accumulate in the cavities and thus reduce the abrasive wear. When slid against the smooth steel surface, the addition of viscose fibers had slight effect on wear rates of the samples (Fig. 19 B1). In the abrasive wear environment (Fig. 19 B2), the high VF-content reduced significantly wear of the specimens, whose sparsely located micro-pillars (SC15-SC35) enabled debris to accumulate into the cavities. Reduced wear originated from the higher stiffness of the composite material (Table 2).

3.2. Influence of surface structuring on adhesion of aluminum-polymer resin joints [II, III]

The main objective of the following studies was to improve adhesion and hence the mechanical strength of the aluminum-polymer resin joints mainly by fabricating micro- and nanoscale surface structures on the aluminum substrate. Surface structuring was performed to increase the area of adhesion interface and to promote mechanical interlocking.[66,73,72,] The effects of chemical and energetic modifications were also investigated because according to the generally accepted adsorption theory, a chemical interaction between the adherend and adhesive is known to have a great influence on adhesion.[66,72]

3.2.1. Surface structures [II, III]

The surfaces of aluminum adherends were structured on microscale by using micro-mesh printing technique and sandblasting. The dimensions of the structured area were 25 mm * 15 mm. Micro-mesh printing was performed by using stainless steel meshes with mesh sizes of 100 µm, 200 µm and 400 µm. The micro-mesh printing and sandblasting were also combined in order to achieve different micro-micro-hierarchical surface patterns. The names and fabrication sequences of the microscale surface specimens are listed in Table 4. After the fabrication, the surface patterns were evaluated by using SEM imaging. The examples of the fabricated surface structures are shown in Figure 20.

Table 4. Fabricated microscale surface structures of aluminum substrates.

Surface	Abbreviation	1. treatment	2. treatment
Smooth	Smooth	-	-
Sandblasted	S	Sandblasting	-
Mesh printed	M^{100} * M^{200} M^{400}	Micro-mesh printing	-
Sandblasted + mesh printed	SM^{100} SM^{200} SM^{400}	Sandblasting	Micro-mesh printing
Mesh printed + sandblasted	$M^{100}S$ $M^{200}S$ $M^{400}S$	Micro-mesh printing	Sandblasting

* Numbers indicate mesh size, e.g. M^{100} equals to 100 µm mesh print structure.

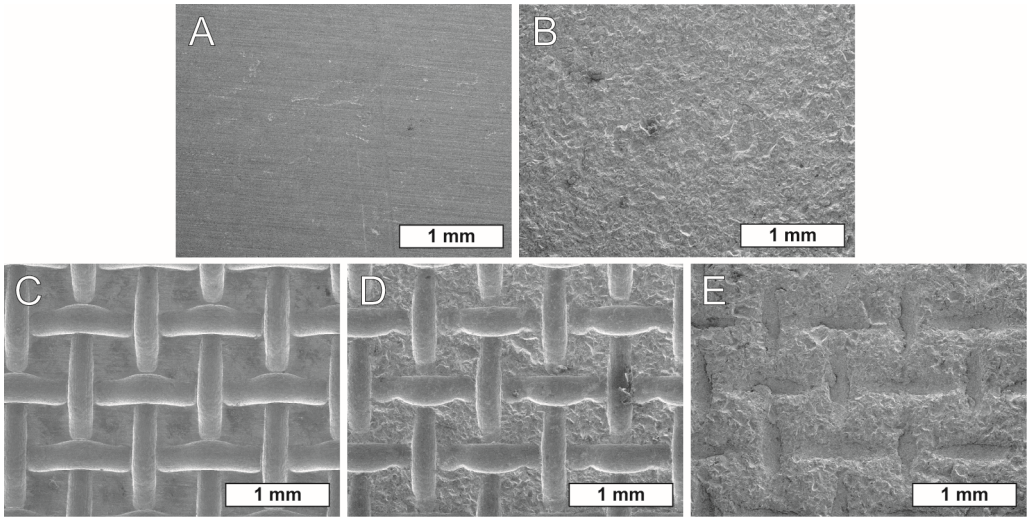

Figure 20. SEM images of the A) smooth, B) sandblasted, C) M^{400}, D) SM^{400} and E) $M^{400}S$ surfaces.[II,III]

Some smooth, sandblasted, M^{100} and $M^{400}S$ aluminum specimens were modified with nanoscale surface structures. The nanoscale pseudoboehmite (AlO(OH), a crystalline form of Al_2O_3) surface structure was obtained via hydration by using boiling water treatment. The nanoscale surface structure was combined with the microscale surface structures to achieve superimposed micro-nano and micro-micro-nano surface structures. The formed pseudoboehmite nanostructures were then evaluated with SEM imaging (see Figure 21).

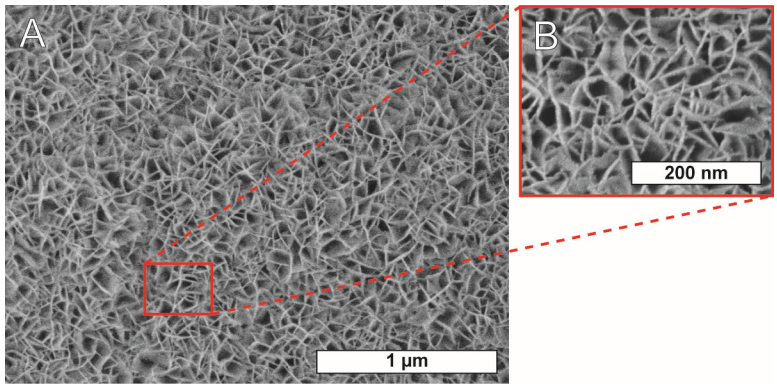

Figure 21. A) SEM image of pseudoboehmite nanostructure obtained with 5 min hydration and B) close-up of the structure.[III]

3.2.2. Functionalization of the aluminum surface [II, III]

To enhance the chemical interaction between aluminum and polymer resin, the aluminum surfaces were functionalized with silanization and plasma treatment. Silanes were hydrolyzed in ethanol solutions containing 5 vol-% of water.[II,III] Five different silane concentrations (0.5-2.5 w-%) were studied in order to achieve the optimal silanization conditions. Plasma treatment of the aluminum adherends was performed with a chamber plasma device in reactive ion etching mode (RIE) with O_2/Ar-gas mixtures acting as the reactive gases.[II] In order to achieve optimal oxygen-level on the aluminum surface, the oxygen content in the reaction gas was varied between 0-40 vol-%. Plasma treatment and silanization conditions were optimized in order to study the effect of combined modifications in further studies.

In aluminum-epoxy composite joints, the optimal oxygen content of plasma gas was found to be 20 %. At best, the plasma treatment improved the shear strength with 24 %, but the adhesive fracture mechanism did not differ from the unmodified specimen. In silanization studies, a decreasing concentration of 3-glycidoxypropyltrimethoxysilane (GPTMS) resulted in increasing shear strength. Silanization with GPTMS improved adhesion up to 68 % and microscale shear cuts started to appear on the fracture surfaces of epoxy.[II] The obtained shear strength results of the plasma and the silane treatments agreed with the previous results reported for metal-epoxy adhesive joints, where adherends have been treated with plasma or silane.[104,106,121]

In aluminum-UP composite joints, the silanization with 3-methacryloxypropyl-trimethoxysilane (MPS) approximately doubled the shear strength, but the concentration of the MPS solution had no significant effect on the shear strengths.[III] The near 100% improvement in shear strength correlated well with the mechanical strength results obtained for the unsaturated polyester resin specimens reinforced with MPS treated Al_2O_3 nanoparticles.[122]

3.2.3. Shear strength of aluminum-epoxy joints [II]

The shear strength values measured for microstructured Al/epoxy/Al-specimens are gathered in Figure 22. The SM-type surface structures (obtained with sandblasting followed by micro-mesh printing) gave lower shear strength values when compared to the mere sandblasted reference structure. The lower shear strength was due to the micro-mesh printing which smoothened the structure produced by sandblasting.[II] Thus, their results are not shown in this thesis.

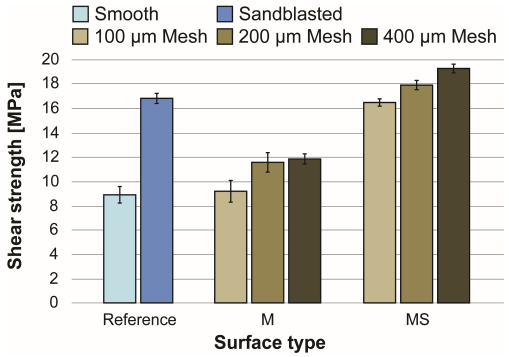

Figure 22. Effect of microstructuring on shear strength of aluminum-epoxy joints.

When compared to smooth reference, the sandblasting, which produces random surface structure, almost doubles the shear strength whereas with the more controlled M-type surfaces the improvement is 33 % at best. Although the small mesh structures should have provided more locking points and hence higher adhesion between epoxy and aluminum (See Paper II, Appendix A), the observed shear strength values for the M-type surfaces showed the reversed trend. This could be explained on the basis of SEM images of the fractured specimens (Fig. 23). All of the M-type specimens had air cavities between epoxy and mesh structure dents (Fig. 23 2C). Especially with the smallest mesh structures, epoxy was not able to wet the surface completely, resulting in a lower effective contact area and hence lower adhesion.

The highly hierarchical $M^{400}S$ surface structure was found to have highest adhesion to epoxy of the studied surface structures. The fracture analysis showed that the $M^{400}S$ structure resulted in more cohesive failure mode (Fig. 23 2D) whereas with the smooth and the M-type surfaces the failure mode was mainly adhesive (Figs. 23 A and C).

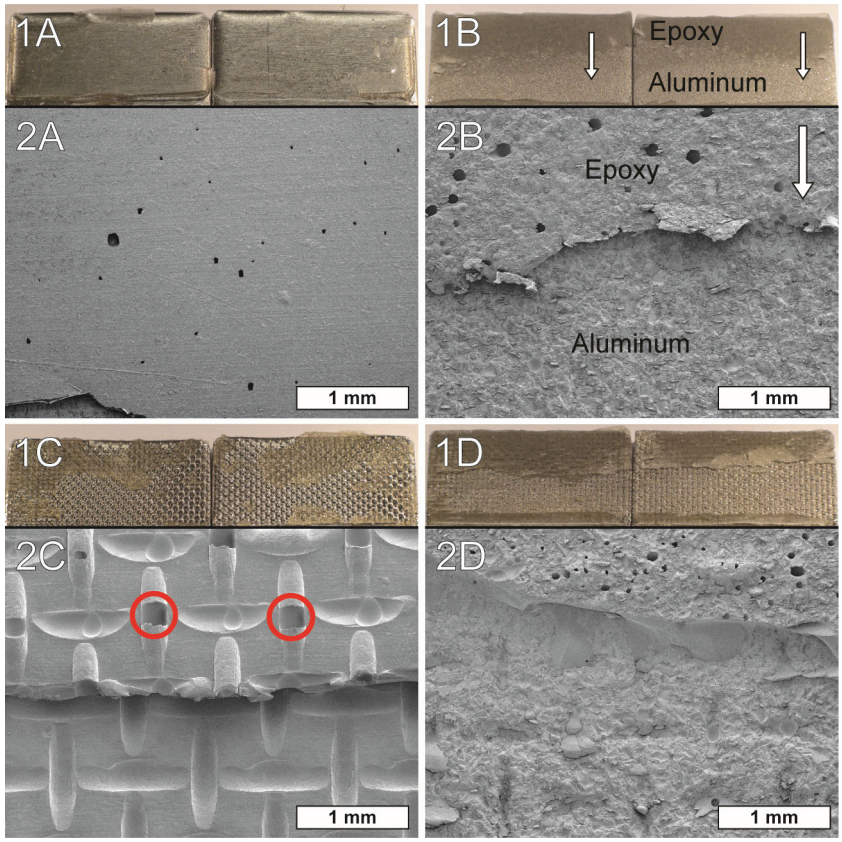

Figure 23. SEM images of fractured A) smooth reference, B) sandblasted reference, C) M^{400} and D) $M^{400}S$ structured Al/epoxy/Al specimen. White arrows indicate the direction of stress. Red circles mark the air cavities between epoxy and the mesh structure dents.

The smooth, sandblasted, M^{400} and $M^{400}S$ structured surfaces were combined with plasma and silane treatments in order to study the effects of combined mechanical and chemical modifications of aluminum substrates on the shear strength. The shear strength values of the combined modifications are shown in Figure 24.

The shear strength results indicated a clear trend, where the higher number of surface modifications resulted in higher shear strength. When the surface chemistry of the aluminum adherends were altered with plasma or silane treatments, the chemical interaction between epoxy and aluminum was enhanced significantly. The improved chemical interaction can be easily seen in Figure 25, where the combined plasma and silane treatment has enhanced the wetting properties of the aluminum surface (no large air cavities) and resulted in a higher extent of cohesive failure. On the $M^{400}S$ surface structures, the combined modifications generated such a high adhesion that the joint specimens started to deflect during the shear testing. The $M^{400}S$ specimens having combined plasma and silane modifications were therefore facing high peeling forces[119], which prevented the evaluation of the maximum shear strength[II]. For clarity, their shear strength results were omitted from the data set in Figure 24.

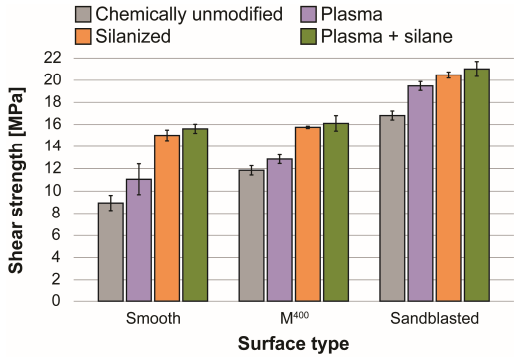

Figure 24. Effect of combined surface modifications methods on shear strengths of aluminum-epoxy joints.

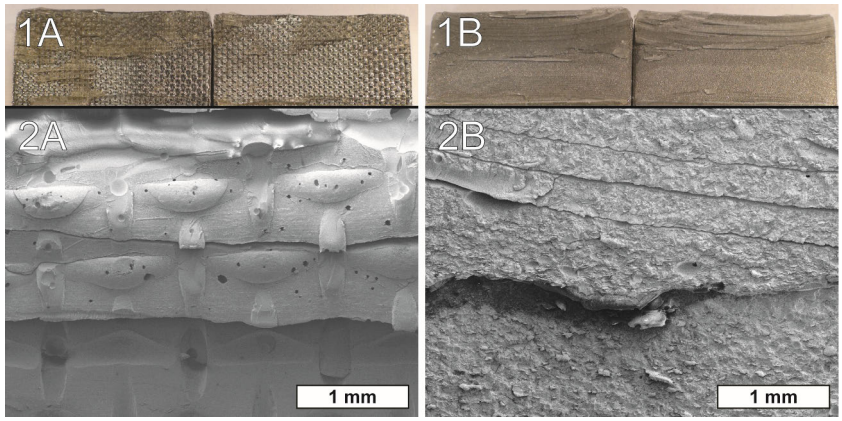

Figure 25. SEM images of fractured plasma + silane modified A) M^{400} structured and B) sandblasted Al/epoxy/Al specimen.

3.2.4. Shear strength of aluminum-UP joints [III]

Based on the good results observed for the aluminum-epoxy joints, the effect of surface structuring on adhesion between aluminum and unsaturated polyester resin was further studied. Due to the low viscosity, UP adhesive was expected to offer good wetting and impregnation properties, thus enabling to examine even the nanoscale surface structures and their function in adhesion promotion. The shear strengths of the micropatterned specimens and the specimens having superimposed micro-nano and micro-micro-nano surface structures are shown in the Figs. 26 A and B.

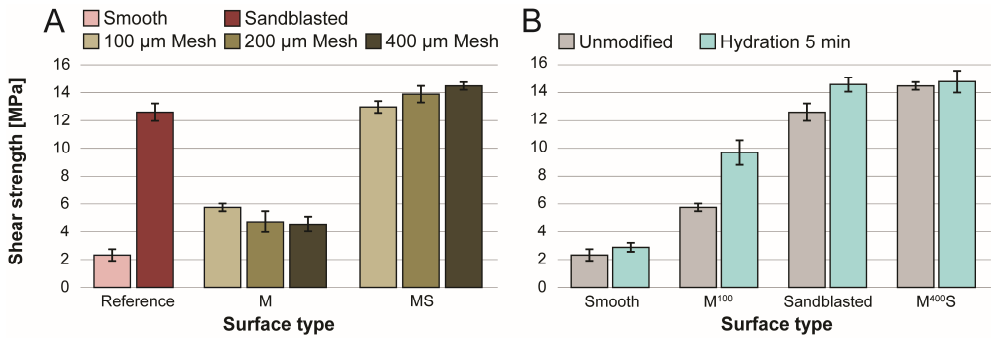

Figure 26. Effects of A) microstructuring and B) hydration on shear strengths of microstructured aluminum adherends in aluminum-UP joints.

Like in the case of aluminum-epoxy composite joints[II], the hierarchical $M^{400}S$ structure produced high adhesion properties when compared to any other microstructures studied (Fig. 26 A). M-type surface structures, however, behaved differently when compared to those studied in the aluminum-epoxy composite joints[II]. Due to the better impregnation property of UP adhesive, the smaller mesh structures on the aluminum adherend generated a higher effective interface area and higher number of locking points, thus increasing the shear strength.

On its own, the pseudoboehmite nanostructure obtained via hydration did not enhance adhesion, but when the nanostructure was combined with the microstructures, a clear improvement was observed (Fig. 26 B). The formed superimposed micro-nano surface structures had up to 1.7 times higher adhesion to UP when compared to the corresponding microstructures. Aluminum-UP joints having three-level micro-micro-nano surface structures on the aluminum substrates had so high adhesion that they deflected during the shear measurements, thus preventing the evaluation of the maximum shear strength.

Photographing under UV-light was found to be a very effective way to investigate the fracture surfaces of the aluminum-UP specimens. The UV-light caused cured polyester adhesive to emit fluorescent light which made the adhesive residues more visible. Figure 27 shows how a nanostructure on a microstructure leads to a more cohesive failure, detected as wide-ranging polyester residues on the exposed aluminum surface.

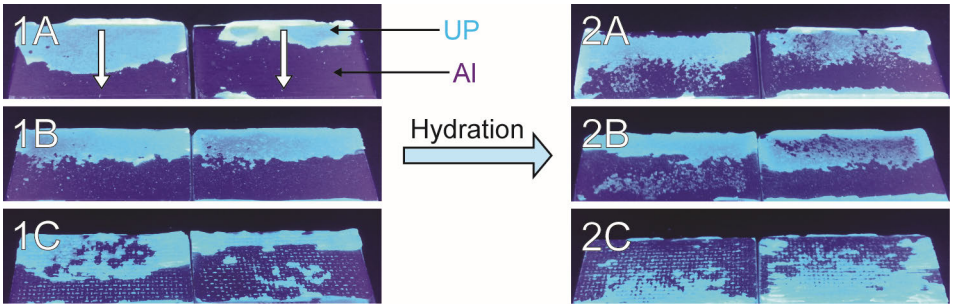

Figure 27. Photographs of fractured A) M^{100}, B) sandblasted and C) $M^{400}S$ Al/UP/Al specimen without (1) and with (2) the nanostructuring obtained via hydration. White arrows indicate the direction of stress.

High adhesion achieved in the micro-micro-nanostructured specimens caused the specimens to deflect and most of UP adhesive to peel off. The majority of the adhesive residues are concentrated on the opposite end of the joint area (Figure 27 2C) when compared to any other studied Al/UP/Al-specimen modified with mechanical and/or hydration methods. SEM imaging of the fractured specimens showed only minor differences between the nanostructured and non-nanostructured specimens, the former ones having slightly more cohesive failure. Examples of the SEM images are shown in the Figure 28.

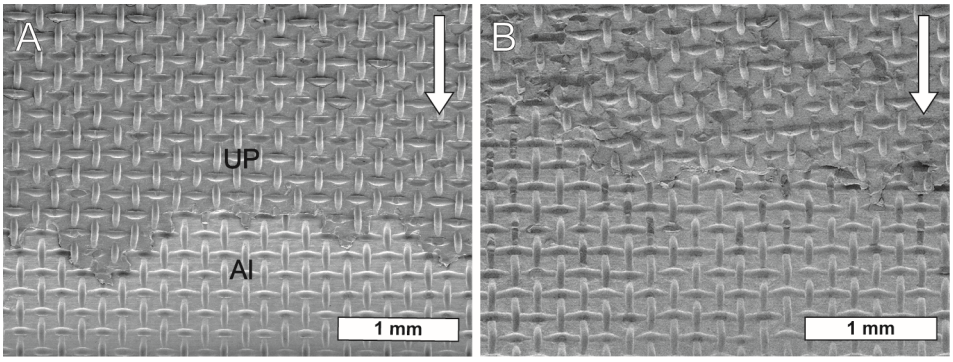

Figure 28. SEM images of fractured M^{100} structured Al/UP/Al specimen without (A) and with (B) the nanostructuring obtained via hydration. White arrows indicate the direction of stress.

A high magnification SEM study of the fractured nanostructured specimens revealed how UP adhesive was not able to penetrate into the nanostructure covering sandblasted microstructure (Fig. 29 A). In order to promote chemical interaction between the nanostructure and UP adhesive, the aluminum substrates were silanized with MPS. Silanization of the aluminum adherends significantly improved wetting of the nanostructure with UP adhesive (Fig 29 B).

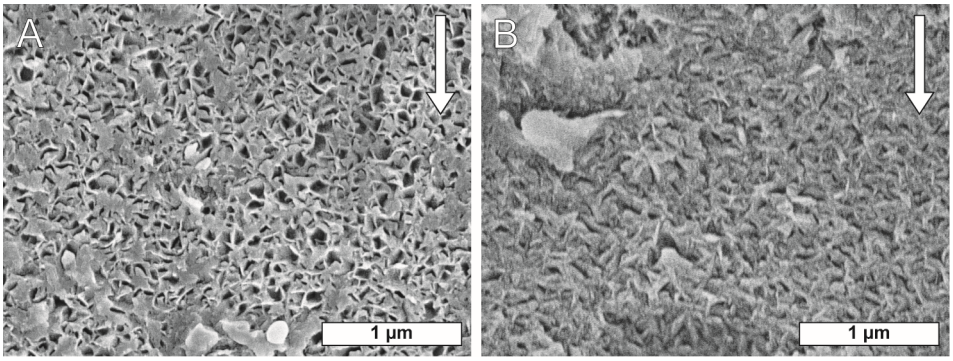

Figure 29. SEM images of exposed pseudoboehmite nanostructure of fractured sandblasted + hydrated Al/UP/Al specimen without (A) and with (B) silanization with MPS.

The enhanced chemical interaction between aluminum and UP improved the penetration of adhesive into the pseudoboehmite nanostructure (Figure 29). The improved penetration resulted in noticeable increase in shear strengths of the Al/UP/Al specimens. The shear strength values of the studied silane treated specimens having micro-, nano- and micro-nanostructures are collected in Figure 30.

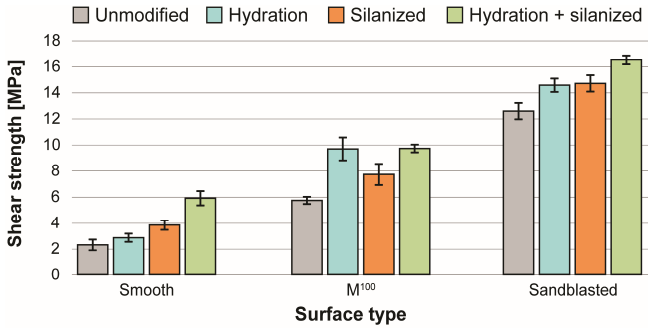

Figure 30. Effect of combined microstructuring, nanostructuring and silanization on shear strength of aluminum-UP joints.

Figure 30 indicates how shear strengths of mere silanization and mere hydration treated aluminum-UP joints differ slightly when compared to each other. On all of the smooth and microstructured surfaces, the combined hydration + silane modification generated the highest adhesion. The improved adhesion properties were due to the enhanced wetting of the hydrated pseudoboehmite structures, which resulted in more effective mechanical locking, a larger contact area and a better chemical interaction on the aluminum-UP interface.

4. Conclusions

The main target in this thesis was to optimize surface structures that could modify the tribological and interfacial adhesion properties of polypropylene/viscose fiber (PP/VF) composites and aluminum-polymer resin composite joints. A wide series of micro- and nanometer scale surface structures was fabricated both on the PP/VF-composites and on the aluminum. The surface structures of the PP/VF-composites were manufactured by means of injection molding with the microstructured mold inserts. The surface structuring of the aluminum adherends was performed with direct methods (micro-mesh printing, sandblasting and hydration). All of the studied surface structuring methods were chosen due to their easy scalability to mass-production.

The increasing fiber content enhanced the mechanical properties of the PP/VF-composites and decreased friction and wear of the specimens during the dry sliding. The micro-pillar structuring of the PP/VF-composites was found to significantly enhance the stability of sliding friction. This was due to the cavities between the micro-pillars where wear debris was able to accumulate. With a proper selection of the micro-pillar array, wear of the PP/VF-composites was notably reduced especially in the abrasive wear environment.

Micropatterning of the aluminum adherends was observed to increase the shear strength of the fabricated aluminum-polymer resin composite joints considerably. The impregnation properties of polymer resins determined the size of the micropatterns that can be used in order to achieve enhancement in adhesion. Hierarchical micro-microstructures had excellent adhesion effects with both of the studied epoxy and unsaturated polyester (UP) resins. Nanoscale surface structuring was found to enhance adhesion between UP and aluminum when the nanostructure was combined with microstructures in a form of superimposed micro-nano- and micro-micro-nanostructures.

By altering the chemistry of the aluminum adherends via plasma treatment or silanization, a considerable improvement in the wetting and impregnation was observed with both of studied adhesives. The more suitable chemical environment attracted adhesives into the fabricated micro- and nano-cavities that further improved adhesion.

As a summary, it can be concluded that the surface patterning is a suitable method to enhance the tribological and interfacial adhesion properties of different composite systems. In order to fully benefit from the surface structures, a suitable chemical modification is also needed. When a proper surface structure is combined with an appropriate chemical modification, the interfacial adhesion properties of aluminum with thermosetting resins can be improved significantly.

The obtained results give a good platform to be utilized especially in the transportation industry where robust and reliable composite materials and joints are required since failures can have catastrophic consequences. The composite joint research could be continued by examining the potential of the optimized system for utilization in other adhesive and substrate systems.

Acknowledgements

This study was carried out at the Department of Chemistry, University of Eastern Finland, during the years 2010-2015 within PRI project, SAM project and Inorganic Materials Chemistry Graduate Program (EMTKO). Financial support from the Finnish Funding Agency for Technology and Innovation (Tekes), EMTKO and the European Union/European Regional Development Fund (ERDF) are gratefully acknowledged.

I am deeply grateful to my supervisors, Prof. Tuula Pakkanen and Prof. Mika Suvanto for the opportunity to work and study in the captivating field of material chemistry. Their solid expertise, professional guidance and unwavering support during the years have been invaluable.

I would like to thank my office mates Ville Nissinen, Dr. Markus Erola and Dr. Tarmo Korpela for offering such an entertaining and encouraging working environment. A special thanks goes to Dr. Tarmo for his valuable collaboration work and scientific discussions. As a whole, I also thank the research group of Materials chemistry for a pleasant work community and especially Päivi Inkinen to keep us on an adequately short leash in the lab.

A warm thank goes to my apprentices Aapo, Samson, Rezaul, Henri and Jani for their valuable work in the field of adhesive joints. I learned at least as much from you guys as you learned from me. I also want to acknowledge Martti Lappalainen, who has been materializing the countless "latest plans" that me and my apprentices have had.

I want also to acknowledge the "meeting of the sediment"-group with whom I have spent countless "scientific" meetings and drank too much coffee.

Heartwarming thanks goes to my fellow students Tuire and Marjo for taking me under their protective grasp. You two don't know how much your company with bad jokes really meant to me when I came back to University. All the numerous movie nights which we have spent with Miika and Mika have offered a superb way to relax during the studies.

My most heartfelt gratitude to the people who have absolutely no clue what I have been doing the past years. My sisters, parents and friends have offered great amount of support and given a precious counterbalance to the studies.

Joensuu, September 2015 *Janne Salstela*

References

[1] V. Kurri, T. Malén, R. Sandell, M. Virtanen, *Muovitekniikan perusteet*, 2nd edition, Hakapaino OY, Helsinki, 2000

[2] Z. Tadmor, C.G. Gogos, *Principles of polymer processing*, 2nd edition, John Wiley & sons, USA, 2006

[3] K. Friedrich, S. Fakirov, Z. Zhang, *Polymer composites: from nano- to micro-scale*, Springer, USA, 2005

[4] W.D. Callister, D.G. Rethwisch, *Materials Science and Engineering*, 9th edition, John Wiley & sons, Asia, 2015, p. 11

[5] Ibid. p. 540

[6] Y.T. Cheng, D.E. Rodak, C.A. Wong, C.A. Hayden, *Effects of micro- and nano-structures on the self-cleaning behaviour of lotus leaves*, Nanotechnology 17 (2006), p. 1359-1362

[7] T. Sun, L. Feng, X. Gao, L. Jiang, *Bioinspired surfaces with special wettability*, Accounts of Chemical Research 38 (2005), p. 644-652

[8] W. Barthlott, C. Neinhuis, *Purity of the sacret lotus, or escape from contamination in biological surfaces*, Planta 202 (1997), p. 1-8

[9] D. Zhao, Q. Tian, M. Wang, Y. Jin, *Study on the hydrophobic property of shark-skin-inspired micro-riblets*, Journal of Bionic Engineering 11 (2014), p. 296-302

[10] H. Chen, X. Zhang, L. Ma, D. Che, D. Zhang, T.S. Sudarshan, *Investigation on large-area fabrication of vivid shark skin with superior surface functions*, Applied Surface Science 316 (2014), p. 124-131

[11] D.G. Stavenga, S. Foletti, G. Palasantzas, K. Arikawa, *Light on the moth-eye corneal nipple array of butterflies*, Proceedings of the Royal Society B: Biological Sciences 273 (2006), p. 661-667

[12] H. Gao, X. Wang, H. Yao, W. Artz, *Mechanics of hierarchical adhesion structures of geckos*, Mechanics of materials 37 (2005), p. 275-285

[13] H. Yao, H. Gao, *Mechanics of robust and releasable adhesion in biology: Bottom-up designed hierarchical structures of gecko*, Journal of the Mechanics and Physics of Solids 54 (2006), p. 1120-1146

[14] A. Gasparetto, T. Seidl, R. Vidoni, *A Mechanical model for the adhesion of spiders to nominally flat surfaces*, Journal of Bionic Engineering 6 (2009), p. 135-142

[15] T. Korpela, M. Suvanto, T.T. Pakkanen, *Friction and wear of periodically micro-patterned polypropylene in dry sliding*, Wear 289 (2012), p. 1-8

[16] T. Korpela, M. Suvanto, T.T. Pakkanen, *Wear and friction behavior of polyacetal surfaces with micro-structure controlled surface pressure*, 328-329 (2015), p. 262-269

[17] L.F. da Silva, N. Ferreira, V. Richter-Trummer, E. Marques, *Effect of grooves on the strength of adhesively bonded joints*, International Journal of Adhesion & Adhesives 30 (2010), p.735-743

[18] J. Zebala, P. Ciepka, A. Reza, R. Janczur, *Influence of rubber compound and tread pattern of retreaded tyres on vehicle active safety*, Forensic Science International 167 (2007), p. 173-180

[19] H.J. Ensikat, P. Ditsche-Kuru, C. Neinhuis, W. Barthlott, *Superhydrophobicity in perfection: The outstanding properties of the lotus leaf*, Beilstein Journal of Nanotechnology 2 (2011), p. 152-161

[20] C.A. Harper, *Handbook of plastics, elastomers and composites*, fourth edition, McGraw-Hill, New York, 2002, p. 3-6

[21] M. Chanda, S. K. Roy, *Plastic technology handbook*, 2nd edition, Marcel Dekker Inc., New York, 1993, p. 26-30, 34-37

[22] C.W.J. Berendsen, M. Škereňb, D. Najdekb, F. Černýc, *Superhydrophobic surface structures in thermoplastic polymers by interference lithography and thermal imprinting*, Applied Surface Science 255 (2009), p. 9305-9310

[23] C.P. Migliaccio, N. Lazarus, *Fabrication of hierarchically structured superhydrophobic PDMS surfaces by Cu and CuO casting*, Applied Surface Science 353 (2015), p. 269-274

[24] E. Huovinen, J. Hirvi, M. Suvanto, T.A. Pakkanen, *Micro-micro hierarchy replacing micro-nano hierarchy: A precisely controlled way to produce wear-resistant superhydrophobic polymer surfaces*, Langmuir 28 (2012), p. 14747-14755

[25] E. Huovinen, L. Takkunen, T. Korpela, M. Suvanto, T.T. Pakkanen, T.A. Pakkanen, *Mechanically robust superhydrophobic polymer surfaces based on protective micropillars*, Langmuir 30 (2014), p. 1435-1443

[26] L.W. Hea, S.P. Yanc, J.R. Chu, *Directional adhesion of gecko-inspired two-level fibrillar structures*, European Journal of Mechanics - A/Solids 47 (2014), p. 246-253

[27] M. Li, A. Zhaoa, R. Jiang, D. Wang, D. Li, H. Guo, W. Tao, Z. Gan, M. Zhang, *Regulation of the elastic modulus of polyurethane microarrays and its influence on gecko-inspired dry adhesion*, Applied Surface Science 257 (2011), p. 3336-3340

[28] M.L.B. Palacio, B. Bhushan, S.R. Schricker, *Gecko-inspired fibril nanostructures for reversible adhesion in biomedical applications*, Materials Letters 92 (2013), p. 409-412

[29] A.Y.Y. Ho, L.P. Yeo, Y.C. Lam, I. Rodríguez, *Fabrication and analysis of gecko-inspired hierarchical polymer nanosetae*, ACS Nano 5 (2011), p. 1897-1906

[30] H.-K. Koponen, I. Saarikoski, T. Korhonen, M. Pääkkö, R. Kuisma, T.T. Pakkanen, M. Suvanto, T.A. Pakkanen, *Modification of cycloolefin copolymer and poly(vinyl chloride) surfaces by superimposion of nano- and microstructures*, Applied Surface Science 253 (2007), p. 5208-5213

[31] W. *Han*, D. *Wu*, W. *Ming*, J.W. Niemantsverdriet, P.C. Thüne, *Direct catalytic route to superhydrophobic polyethylene films*, Langmuir 22 (2006), p. 7956-7959

[32] B. Cortese, S. D'Amone, M. Manca, I. Viola, R. Cingolani, G. Gigli, *Superhydrophobicity due to the hierarchical scale roughness of PDMS surfaces*, Langmuir 24 (2008), p. 2712-2718

[33] E. Puukilainen, T. Rasilainen, M. Suvanto, T.A. Pakkanen, *Superhydrophobic polyolefin surfaces: Controlled micro- and nanostructures*, Langmuir 23 (2007), p. 7263-7268

[34] J. Gao, Y. Liu, H. Xu, Z. Wang, X. Zhang, *Mimicking biological structured surfaces by phase-separation micromolding*, Langmuir 25 (2009), p. 4365-4369

[35] S.M. Lee, T.H. Kwon, *Mass-productive reblication of highly hydrophobic surfaces from plant leaves*, Nanotechnology 17 (2006), p. 3189-3196

[36] V. Prysiazhnyi, P. Slavicek, M. Cernak, *Aging of plasma-activated copper and gold surfaces and its hydrophilic recovery after water immersion*, Thin Solid Films 550 (2014), p. 373-380

[37] L. Bónová, A. Zahoranová, D. Kováčik, M. Zahoran, M. Mičušík, , M. Černák, *Atmospheric pressure plasma treatment of flat aluminum surface*, Applied Surface Science 331 (2015), p. 79-86

[38] H.-J. Choi, J.-H. Shin, S. Choo, S.-W. Ryu, Y.-D. Kim, H. Lee, *Fabrication of superhydrophobic and oleophobic Al surfaces by chemical etching and surface fluorination*, Thin Solid Films 585 (2015), p. 76-80

[39] S.Z. Saifaldeen, K.R. Khedir, M.F. Cansizoglu, T. Demirkan, T. Karabacak, *Superamphiphobic aluminum alloy surfaces with micro and nanoscale hierarchical roughness produced by a simple and environmentally friendly technique*, Journal of Materials Science 49 (2014), p. 1839-1853

[40] X. Fu, X. He, *Fabrication of super-hydrophobic surfaces on aluminum alloy substrates*, Applied Surface Science 255 (2008), p. 1776-1781

[41] A.K. Bledzki, J. Gassan, *Composites reinforced with cellulose based fibres*, Progress in Polymer Science 24 (1999), p. 221-2747

[42] S. Kalia, K. Thakur, A. Celli, M.A. Kiechel, C.L. Schauer, *Surface modification of plant fibers using environment friendly methods for their application in polymer composites, textile industry and antimicrobial activities: A review,* Journal of Environmental Chemical Engineering 1 (2013), p. 97-112

[43] H. Fan, X. Yu, Y. long, X. Zhang, H. Xiang, C. Duan, N. Zhao, X. Zhang, J. Xu, *Preparation of kapok-polyacrylonitrile core-shell composite microtube and its application as gold nanoparticles carrier*, Applied Surface Science 258 (2012), p. 2876-2882

[44] L.Y. Mwaikambo, E.T.N. Bisanda, *The performance of cotton-kapok fabric-polyester composites*, Polymer Testing 18 (1999), p. 181-198

[45] F.G. Torres, R.M. Diaz, *Morphological characterization of natural fiber reinforced thermoplastics (NFRTP) processed by extrusion, compression and rotational moulding*, Polymers and Polymer Composites 12 (2004), p. 705-718

[46] G.I. Williams, R.P. Wool, *Composites from plant fibers and soy oil resins*, Applied Composite Materials 7 (2000), p. 421-432

[47] A.C. Milanese, M.O.H. Cioffi, H.J.C. Voorwald, *Thermal and mechanical behavior of sisal/phenolic composites*, Composites Part B 4 (2012), p. 2843-2850

[48] A. Belaadi, A. Bezazi, M. Maache, F. Scarpa, *Fatigue in sisal fiber reinforced polyester composites: Hysteresis and energy dissipation*, Procedia Engineering 74 (2014), p. 325-328

[49] H. Sixta, H. Harms, S. Dapia, J.C. Parajo, J. Puls, B. Saake, H.-P. Fink, T. Röder, *Evaluation of new organosolv dissolving pulps. Part I: Preparation, analytical characterization and viscose processability*, Cellulose 11 (2004), p. 73-83

[50] X. Zhang, B.L. Weeks, *Preparation of sub-micron nitrocellulose particles for improved combustion behavior*, Journal of Hazardous Materials 268 (2014), p. 224-228

[51] J. Ganster, H.-P Fink, M. Pinnow, *High-tenacity man-made cellulose fibre reinforced thermoplastics— Injection moulding compound with polypropylene and alternative matrices*, Composites Part A 37 (2006), p. 1796-1804

[52] P. Wambua, J. Ivens, I. Verpoest, *Natural fibres: Can they replace glass in fibre reinforced plastics?*, Composite Science and Technology 63 (2003), p. 1259-1264

[53] W. Bai, K. Li, *Partial replacement of silica with microcrystalline cellulose in rubber composites*, Composites Part A 40 (2009), p. 1597-1605

[54] F.M. AL-Ogla, S.M. Sapuan, *Natural fiber reinforced polymer composites in industrial applications: Feasibility of date palm fibers for sustainable automotive industry*, Journal of Cleaner Production 66 (2014), p. 347-354

[55] O. Faruk, A.K. Bledzki, H.-P. Fink, M. Sain, *Biocomposites reinforced with natural fibers: 2000–2010*, Progress in Polymer Science 37 (2012), p. 1552-1596

[56] V.K. Thakura, M.K. Thakur, R.K. Gupta, *Review: Raw natural fiber–based polymer composites*, International Journal of Polymer Analysis and Characterization 19 (2014), p. 256-271

[57] C. Alves, P. Ferrão, A. Silva, L. Reis, M. Freitas, L. Rodrigues, D. Alves, *Ecodesign of automotive components making use of natural jute fiber composites*, Journal of Cleaner Production 18 (2010), p. 313-327

[58] Z.N. Azwa, B.F. Yousif, A.C. Malano, W. Karunasena, *A review on the degradability of polymeric composites based on natural fibres*, Materials and Design 47 (2013), p. 424-442

[59] M.-P. Ho, H. Wang, J.-H. Lee, C.-K. Ho, K.-T. Lau, J. Leng, D. Hui, *Critical factors on manufacturing process of natural fibre composites*, Composites Part B 43 (2012), p. 3549-3562

[60] T. Paunikallio, J. Kasanen, M. Suvanto, T.T. Pakkanen, *Influence of maleated polypropylene on mechanical properties of composite made of viscose fiber and polypropylene*, Journal of Applied Polymer Science 87 (2003), p. 1895-1900

[61] T. Paunikallio, M. Suvanto, T. T. Pakkanen, *Composition, tensile properties, and dispersion of polypropylene composites reinforced with viscose fibers*, Journal of Applied Polymer Science 91 (2004), p. 2676-2684

[62] T. Paunikallio, M. Suvanto, T. T. Pakkanen, *Grafting of 3-(trimethoxysilyl)propyl methacrylate onto polypropylene and use as a coupling agent in viscose fiber/polypropylene composites*, Reactive and Functional Polymers 68 (2008), p.797-808

[63] S. Mishra, J.B. Naik, Y.P. Patil, *The compatibilising effect of maleic anhydride on swelling and mechanical properties of plant-fiber-reinforced novolac composites*, Composite Science and Technology 60 (2000), p. 1729-1735

[64] A. Valadez-Conzalez, J.M. Cervantes-Uc, R. Olayo, P.J. Herrera-Franco, *Chemical modification of henequen fibers with an organosilane coupling agent*, Composites Part B 30 (1999), p. 321-331

[65] V. Tserki, N.E. Zafeiropoulos, F. Simon, C. Panayiotou, *A study of the the effect of acetylation and propionylation surface treatments on plant fibers*, Composite part A 36 (2005), p. 1110-1118

[66] F. Awaja, M. Gilbert, G. Kelly, B. Fox, P.J. Pigram, *Adhesion of polymers*, Progress in Polymer Science 34 (2009), p. 948-968

[67] S.Y. Park, W.J. Choi, H.S. Choi, H. Kwon, S.H. Kim, *Recent trends in surface treatment technologies for airframe adhesive bonding processing: a review (1995-2008)*, The Journal of Adhesion 86 (2010), p. 192-221

[68] A. Baldan, *Review: Adhesively-bonded joints and repairs in metallic alloys, polymers and composite materials: Adhesives, adhesion theories and surface pretreatment*, Journal of Material Science 39 (2004), p. 1-49

[69] A. M. Pereira, J.M. Ferreira, F.V. Antunes, P.J. Bártolo, *Analysis of manufacturing parameters on the shear strength of aluminium adhesive single-lap joints*, Journal of Materials Processing Technology 210 (2010), p. 610-617

[70] M.W. Rushfort, P. Bowen, E. McAlpine, X. Zhou, G.E. Thompson, *The effect of surface pretreatment and moisture on the fatigue performance of adhesively-bonded aluminum*, Journal of Materials Process and Technology 153-154 (2004), p. 359-365

[71] T.A. Barnes, I.R Pashby, *Joining techniques for aluminium spaceframes used in automobiles: Part II — Adhesive bonding and mechanical fasteners*, Journal of Materials Processing Technology 99 (200), p. 72-79

[72] A. Baldan, *Adhesion phenomena in bonded joints*, International Journal of Adhesion & Adhesives 38 (2012), p. 95-116

[73] T. Semoto, Y. Tsuji, K.Yoshizawa, *Molecular understanding of the adhesive force between a metal oxide surface and an epoxy resin*, Journal of Physical Chemistry C 115 (2011), p. 11701–11708

[74] C.V Cagle, *Handbook of adhesive bonding*, McGraw-Hill, New York, 1972, p. 114

[75] J. Seppälä, *Polymeeriteknologian perusteet, 3rd edition, Hakapaino Oy, Helsinki, 1999, p.* 115-117*, 126-129*

[76] F.N. Tüzün, M.S. Tunalıoğlu, *The effect of finely-divided fillers on the adhesion strengths of epoxy-based adhesives*, Composite Structures 121 (2015), p. 296-303

[77] M.D. Banea, L.F.M. da Silva, *Adhesively bonded joints in composite materials: An overview*, Proceedings of the Institution of Mechanical Engineers, Part L: Journal of Materials: Design and Applications 223 (2008), p. 1-18

[78] D.S. Lee, C.D. Han, *The effect of resin chemistry on the curing behavior and chemorheology of unsaturated polyester resins*, Journal of Applied Polymer Science 34 (1987), p. 1235-1258

[79] L.G. Batch, C.W. Macosko, *Kinetics model for crosslinking free radical polymerization including diffusion limitations*, Journal of Applied Polymer Science 44 (1992), p. 1711-1729

[80] Y.J. Huanc, C.J. Chen, *Curing of unsaturated polyester resins-effects of comonomer composition. I. Low-temperature reactions*, Journal of Applied Polymer Science 46 (1992), p. 1573-1601

[81] J. Dai, b, S. Ma, X. Liu, L. Han, Y. Wu, X. Dai, J. Zhu, *Synthesis of bio-based unsaturated polyester resins and their application in waterborne UV-curable coatings*, Progress in Organic Coatings 78 (2015), p. 49-54

[82] I. Mironi-Harpaz, M. Narkis, A. Siegmann, *Nanocomposite systems based on unsaturated polyester and organo-clay*, Polymer Engineering & Science 45 (2005), p.147-186

[83] J. Simitzis, D. Triantou, S. Soulis, G. Tsangaris, L. Zoumpoulakis, E. Manolopoulos, *Influence of backbone rigidity on the curing and the dielectric relaxations of unsaturated polyesters*, Journal of Applied Polymer Science 120 (2011), p. 1984-1993

[84] K. Riistama, J. Laitinen, M. Vuori, *Suomen kemian teollisuus*, 5th edition, Chemas Oy, Helsinki, 2003, p. 71

[85] S.G. Prolongo, A. Ureña, *Effect of surface pre-treatment on the adhesive strength of epoxy–aluminium joints*, International Journal of Adhesion & Adhesives 29 (2009), p. 23-31

[86] J. G. Kim, I. Choi ja D. G. Lee, *Contact angle and wettability of hybrid surface-treated metal adherends*, Journal of Adhesion Science and Technology 27 (2013) p. 794-810

[87] A.F. Harris, A. Beevers, *The effects of grit-blasting on surface properties for adhesion*, International Journal of Adhesion & Adhesives 19 (1999), p. 445-452

[88] G.W. Critchlow, D.M. Brewis, *Review of surface treatments for aluminium* alloys, International Journal of Adhesion & Adhesives 16 (1996), p. 255-275

[89] M. Shahid, S.A. Hashim, *Effect of surface roughness on the strength of cleavage joints*, International Journal of Adhesion and Adhesives 22 (2002) p. 235-244

[90] D.G. Lee, J.W. Kwon, D.H, Cho, *Hygrothermal effects on the strength of adhesively bonded joints*, Journal of Adhesion Science and Technology 12 (1998), p. 1253-1275

[91] G.W. Critchlow, K.A. Yendall, D. Bahrani, A. Quinn, F. Andrews, *Strategies for the replacement of chromic acid anodising for the structural bonding of aluminium alloys*, International Journal of Adhesion & Adhesives 26 (2006), p. 419-453

[92] J.S. Zhang, X.H. Zhano, Y. Zuo, J.P. Xiong, *The bonding strength and corrosion resistance of aluminium alloy by anodizing treatment in a phosphoric acid modified boric acid/sulfuric acid bath*, Surface & Coatings Technology 202 (2008), p. 3149-3156

[93] M. Mohseni, M. Mirabedini, M. Hashemi, G.E. Thompson, *Adhesion performance of an epoxy clear coat on aluminum alloy in the presence of vinyl and amino-silane primers*, Progress in Organic Coatings 57 (2006). p. 307-313

[94] F. Deflorian, S. Rossi, L. Fedrizzi, *Silane pre-treatments on copper and aluminium*, Electrochimica Acta 51 (2006), p. 6097-6103

[95] M. Esfandeh, S.M. Mirabedini, M.T. Pazokifard, *Study of silicone coating adhesion to an epoxy undercoat using silane compounds: Effect of silane type and application method*, Colloids and Surfaces A: Physicochemical and Engineering Aspects 302 (2007), p. 11-16

[96] A. Pizzi, K. Mittal (Eds.), Handbook of adhesive technology, 2nd edition, Marcel Dekker, USA, 2003, p. 17

[97] M. Xanthos (Ed.), Functional fillers for plastics, Wiley VCH Verlag, Germany, 2005, p. 59-84.

[98] Y. Xie, C.A.S. Hill, Z. Xiao, H. Militz, C. Mai, *Silane coupling agents used for natural fiber/polymer composites: A review*, Composites Part A: Applied Science and Manufacturing, 41 (2010), p. 806-819

[99] A.P. Pijpers, R.J. Meier, *Adhesion behaviour of polypropylenes after flame treatment determined by XPS (ESCA) spectral analysis*, Journal of Electron Spectroscopy and Related Phenomena 121 (2001), p. 299-313

[100] J.G. Kim, I. Choi, D.G. Lee, I.S. Seo, *Flame and silane treatments for improving the adhesive bonding characteristics of aramid/epoxy composites*, Composite Structures 93 (2011), p. 2696-2705

[101] R. Wolf and A. Sparavigna, *Role of plasma surface treatments on wetting and adhesion*, Engineering 2 (2010), p. 397-402

[102] J.H. Ku, I.H. Jung, K.Y. Rhee, S.J. Park, *Atmospheric pressure plasma treatment of polypropylene to improve the bonding strength of polypropylene/aluminum composites*, Composites Part B: Engineering 45 (2013), p. 1282-1287

[103] N. Saleema, D. Gallant, *Atmospheric pressure plasma oxidation of AA6061-T6 aluminum alloy surface for strong and durable adhesive bonding applications*, Applied Surface Science 282 (2013), p. 98-104

[104] C. Sperandio, J. Bardon, A. Laachachi, H. Aubriet, D. Ruch, *Influence of plasma surface treatment on bond strength behaviour of an adhesively bonded aluminium-epoxy system*, International Journal of Adhesion and Adhesives 30 (2010), p. 720-728

[105] W. Polini, L. Sorrentino, *Adhesion of a protective coating on a surface of aluminium alloy treated by air cold plasma*, International Journal of Adhesion and Adhesives 27 (2007), p. 1-8

[106] J.A. Ting, L.M. Rosario, M.C. Lacdan, H.V Lee, J.C. De Vero, H.J. Ramos, R.B. Tumlos, *Enhanced adhesion of epoxy-bonded steel surfaces using O_2/Ar microwave plasma treatment*, International Journal of Adhesion and Adhesives 40 (2013), p. 64-69

[107] U. Petterson, S. Jacobson, *Friction and wear properties of micro textured DLC coated surfaces in boundary lubricated sliding*, Tribology Letters 17 (2004), p. 553-559

[108] Z. Mane, J.-L. Loubet, C. Guerret, L. Guy, O. Sanseau, L. Odini, L. Vanel, D.R. Long, P. Sotta, *A new rotary tribometer to study wear of reinforced rubber materials*, WEAR 306 (2013), p. 149-160

[109] M.R. Kashani, E. Behazin, A. Fakhar, *Construction and evaluation of a new tribometer for polymers*, Polymer Testing 30 (2011), p. 271-276

[110] S. Zhang, W. Wang, Z. Zhano, *The effect of surface roughness characteristics on the elastic-plastic contact performance*, Tribology International 79 (2014), p. 59-73

[111] Y. Xing, J. Deng, Z. Wu, H. Cheng, *Effect of regular surface textures generated by laser on tribological behavior of Si_3N_4/TiC ceramic*, Applied surface Science 265 (2012), p. 823-832

[112] Sivaraos, T.C. Yapb, Qumrul, M.A. Amran, T.J.S. Anand, R. Izamshah, A.A. Aziz, *Friction performance analysis of waste tire rubber powder reinforced polypropylene using pin-on-disk tribometer*, Procedia Engineering 68 (2013), p. 743-749

[113] M. Geiger, S. Roth, , W. Becker, *Influence of laser-produced microstructures on the tribological behaviour of ceramics*, Surface and Coatings Technology 100-101 (1998), p. 17-22

[114] D. L. Burris, W. G. Sawyer, *Addressing practical challenges of low friction coefficient measurements*, Tribology Letters 35 (2009), p. 17-23

[115] A. Baldan, *Review: Adhesively-bonded joints and repairs in metallic alloys, polymers and composite materials: Mechanical and environmental durability performance*, Journal of Material Science 39 (2004), p. 4729-4797

[116] A. Kimiaeifar, H. Toft, E. Lund, O.T. Thomsen, J.D. Sørensen, *Reliability analysis of adhesive bonded scarf joints*, Engineering Structures 35 (2012), p. 281-287

[117] M. Sautrot, M.-L. Abel, J. F. Watts, J. Powell, *Incorporation of an adhesion promoter in a structural adhesive: Aspects of durability and interface chemistry*, The Journal of Adhesion 81 (2005), p. 163-187

[118] R.D. Adams, J.W. Cowap, G. Farquharson, G.M. Margary, D. Vaughn, *The relative merits of the Boeing wedge test and the double cantilever beam test for assessing the durability of adhesively bonded joints, with particular reference to the use of fracture mechanics*, International Journal of Adhesion and Adhesives 29 (2009), p. 609-620

[119] L.F.M da Silva, P.J.C. das Neves, R.D. Adams, J.K Spelt, *Analytical models of adhesively bonded joint – Part I: Literature survey*, International Journal of Adhesion and Adhesives 29 (2009), p. 319-330

[120] W.D. Callister, D.G. Rethwisch, *Materials science and engineering*, 9th edition, John Wiley & sons, Asia, 2015, p. 210-214

[121] J. Qui, E. Sakai, L. Lei, Y. Takarada, S. Murakami, *Improving the shear strength by silane treatments of aluminum for direct joining of phenolic resin*, Journal of Materials Processing Technology 212 (2012), p. 2406-2412

[122] M. Zhang, R.P. Singh, *Mechanical reinforcement of unsaturated polyester by AL_2O_3 nanoparticles*, Materials Letters 58 (2004), p. 408-412